

Last Revision December 15 2020

**ICE, CLOUD, and Land Elevation Satellite-2
(ICESat-2) Project**

**Algorithm Theoretical Basis Document (ATBD)
For
Land-Ice Along-Track Products Part 2:
Land-ice H(t)/ATL11**

**Prepared By: Benjamin Smith, Suzanne Dickinson
Kaitlin Harbeck, Tom Neumann, David Hancock, Jeffery Lee, Benjamin Jelly**



**Goddard Space Flight Center
Greenbelt, Maryland**

26

Abstract

27

28

CM Foreword

29 This document is an Ice, Cloud, and Land Elevation Satellite-2 (ICESat-2) Project Science
30 Office controlled document. Changes to this document require prior approval of the Science
31 Development Team ATBD Lead or designee. Proposed changes shall be submitted in the
32 ICESat-II Management Information System (MIS) via a Signature Controlled Request (SCoRe),
33 along with supportive material justifying the proposed change.

34 In this document, a requirement is identified by “shall,” a good practice by “should,” permission
35 by “may” or “can,” expectation by “will,” and descriptive material by “is.”

36 Questions or comments concerning this document should be addressed to:

37 ICESat-2 Project Science Office

38 Mail Stop 615

39 Goddard Space Flight Center

40 Greenbelt, Maryland 20771

41

42

Preface

43

44 This document is the Algorithm Theoretical Basis Document for the TBD processing to be
45 implemented at the ICESat-2 Science Investigator-led Processing System (SIPS). The SIPS
46 supports the ATLAS (Advance Topographic Laser Altimeter System) instrument on the ICESat-
47 2 Spacecraft and encompasses the ATLAS Science Algorithm Software (ASAS) and the
48 Scheduling and Data Management System (SDMS). The science algorithm software will produce
49 Level 0 through Level 4 standard data products as well as the associated product quality
50 assessments and metadata information.

51 The ICESat-2 Science Development Team, in support of the ICESat-2 Project Science Office
52 (PSO), assumes responsibility for this document and updates it, as required, as algorithms are
53 refined or to meet the needs of the ICESat-2 SIPS. Reviews of this document are performed
54 when appropriate and as needed updates to this document are made. Changes to this document
55 will be made by complete revision.

56 Changes to this document require prior approval of the Change Authority listed on the signature
57 page. Proposed changes shall be submitted to the ICESat-2 PSO, along with supportive material
58 justifying the proposed change.

59 Questions or comments concerning this document should be addressed to:

60 Thorsten Markus, ICESat-2 Project Scientist
61 Mail Stop 615
62 Goddard Space Flight Center
63 Greenbelt, Maryland 20771

64

65

Review/Approval Page

Prepared by:

Benjamin Smith
Principal Researcher
University of Washington
Applied Physics Lab Polar Science Center
1013 NE 40th Street
Box 355640
Seattle, WA 98105

Reviewed by:

Shane Grigsby
Postdoctoral Scholar
Colorado School of Mines
Department of Geophysics

Ellen Enderlin
Assistant Professor
Department of Geosciences
Boise State University

Approved by:

Tom Neumann
Project Scientist
Code 615

66

67

68

***** Signatures are available on-line at: <https://icesatiimis.gsfc.nasa.gov> *****

Change History Log

Revision Level	Description of Change	SCoRe No.	Date Approved
1.0	Initial Release		
1.1	Changes for release 002. Calculate all crossovers (including near 88 S), determine the center of the y_atc search from the median of unique pair center locations.		

70

List of TBDs/TBRs

Item No.	Location	Summary	Ind./Org.	Due Date

71

72	Table of Contents	
73	Abstract	ii
74	CM Foreword	iii
75	Preface.....	iv
76	Review/Approval Page	v
77	Change History Log	vi
78	List of TBDs/TBRs	vii
79	Table of Contents.....	viii
80	List of Figures	x
81	List of Tables.....	xi
82	1.0 INTRODUCTION.....	1
83	2.0 BACKGROUND INFORMATION and OVERVIEW	2
84	2.1 Background	2
85	2.2 Elevation-correction Coordinate Systems	3
86	2.3 Terminology:	4
87	2.4 Repeat and non-repeat cycles in the ICESat-2 mission	5
88	2.5 Physical Basis of Measurements / Summary of Processing.....	6
89	2.5.1 Choices of product dimensions.....	6
90	2.6 Product coverage	7
91	3.0 ALGORITHM THEORY: Derivation of Land Ice H (t)/ATL11 (L3B).....	8
92	3.1 Input data editing	10
93	3.1.1 Input data editing using ATL06 parameters.....	11
94	3.1.2 Input data editing by slope	12
95	3.1.3 Spatial data editing	13
96	3.2 Reference-Surface Shape Correction.....	14
97	3.2.1 Reference-surface shape inversion	14
98	3.2.2 Misfit analysis and iterative editing	15
99	3.3 Reference-shape Correction Error Estimates	16
100	3.4 Calculating corrected height values for repeats with no selected pairs	17
101	3.5 Calculating systematic error estimates	17
102	3.6 Calculating shape-corrected heights for crossing-track data	18

ICESat-2 Algorithm Theoretical Basis Document for Land Ice H(t) (ATL11)

Release 002

103	3.7	Calculating parameter averages	19
104	3.8	Output data editing.....	19
105	4.0	LAND ICE PRODUCTS: Land Ice H (t)(ATL 11/L3B).....	20
106	4.1.1	File naming convention	20
107	4.2	/ptx group.	20
108	4.3	/ptx/ref_surf group	22
109	4.4	/ptx/cycle_stats group	24
110	4.5	/ptx/crossing_track_data group	26
111	5.0	ALGORITHM IMPLEMENTATION	28
112	5.1.1	Select ATL06 data for the current reference point.....	29
113	5.1.2	Select pairs for the reference-surface calculation.....	29
114	5.1.3	Adjust the reference-point y location to include the maximum number of	
115	cycles	32	
116	5.1.4	Calculate the reference surface and corrected heights for selected pairs	33
117	5.1.5	Calculate corrected heights for cycles with no selected pairs.	36
118	5.1.6	Calculate corrected heights for crossover data points	38
119	5.1.7	Provide error-averaged values for selected ATL06 parameters	39
120	5.1.8	Provide miscellaneous ATL06 parameters	40
121	5.1.9	Characterize the reference surface	41
122	6.0	Appendix A: Glossary	43
123	7.0	Browse products.....	50
124		Glossary/Acronyms.....	56
125		References.....	58
126			

127
128
129
130
131
132
133
134
135
136
137
138
139

List of Figures

<u>Figure</u>	<u>Page</u>
Figure 2-1. ICESat-2 repeat-track schematic.....	3
Figure 2-2. ATL06 data for an ATL11 reference point.....	4
Figure 2-3. Potential ATL11 coverage.....	7
Figure 3-1. ATL11 fitting schematic.....	8
Figure 3-2. Data selection.....	11
Figure 5-1 Flow Chart for ATL11 Surface-shape Corrections.....	28
Figure 6-1. Spots and tracks, forward flight.....	47
Figure 6-2. Spots and tracks, backward flight.....	48
Figure 6-3. Granule regions.....	48

140

List of Tables

141

142	<u>Table</u>	<u>Page</u>
143	Table 3-1 Parameter Filters to determine the validity of segments for ATL11 estimates.....	10
144	Table 4-1 Parameters in the <i>/ptx/</i> group.....	21
145	Table 4-2 Parameters in the <i>/ptx/ref_surf</i> group.....	22
146	Table 4-3 Parameters in the <i>/ptx/cycle_stats</i> group.....	24
147	Table 4-4 Parameters in the <i>/ptx/crossing_track_data</i> group.....	26

148

149 **1.0 INTRODUCTION**

150 This document describes the theoretical basis and implementation of the level-3b land-ice
151 processing algorithm for ATL11, which provides time series of surface heights. The higher-level
152 products, providing gridded height, and gridded height change will be described in supplements
153 to this document available in early 2020.

154 ATL11 is based on the ICESat-2 ATL06 Land-ice Height product, which is described
155 elsewhere (Smith and others, 2019a, Smith and others, 2019b). ATL06 provides height estimates
156 for 40-meter overlapping surface segments, whose centers are spaced 20 meters along each of
157 ICESat-2's RPTs (reference pair tracks), but displaced horizontally both relative to the RPT and
158 relative to one another because of small (a few tens of meters or less) imprecisions in the
159 satellite's control of the measurement locations on the ground. ATL11 provides heights
160 corrected for these offsets between the reference tracks and the location of the ATLAS
161 measurements. It is intended as an input for high-level products, ATL15 and ATL16, which
162 will provide gridded estimates of ice-sheet height and height change, but also may be used alone,
163 as a spatially-organized product that allows easy access to height-change information derived
164 from ICESat-2.

165 ATL11 employs a technique which builds upon those previously used to measure short-term
166 elevation changes using ICESat repeat-track data. Where surface slopes are small and the
167 geophysical signals are large compared to background processes (i.e., ice plains and ice shelves),
168 some studies have subtracted the mean from a collection of height measurements from the same
169 repeat track to leave the rapidly-changing components associated with subglacial water motion
170 (Fricker and others, 2007) or tidal flexure (Brunt and others, 2011). In regions where off-track
171 surface slopes are not negligible, height changes can be recovered if the mean height and an
172 estimate of the surface slope (Smith and others, 2009) are subtracted from the data, although in
173 these regions the degree to which the surface slope estimate and the elevation-change pattern are
174 independent is challenging to quantify.

175 ICESat-2's ATL06 product provides both surface height and surface-slope information each time
176 it overflies its reference tracks. The resulting data are similar to that from the scanning laser
177 altimeters that have been deployed on aircraft in Greenland and Antarctica for two decades
178 (cite), making algorithms originally developed for these instruments appropriate for use in
179 interpreting ATLAS data. One example is the SERAC (Surface Elevation Reconstruction and
180 Change Detection) algorithm (Schenk & Csatho, 2012) provides an integrated framework for the
181 derivation of elevation change from altimetry data. In SERAC, polynomial surfaces are fit to
182 collections of altimetry data in small (< 1 km) patches, and these surfaces are used to correct the
183 data for sub-kilometer surface topography. The residuals to the surface then give the pattern of
184 elevation change, and polynomial fits to the residuals as a function of time give the long-term
185 pattern of elevation change. The ATL11 algorithm is similar to SERAC, except that (1)
186 polynomial fit correction is formulated somewhat differently, so that the ATL11 correction gives
187 the surface height at the fit center, not the height residual, and (2) ATL11 does not include a
188 polynomial fit with respect to time.

189

190 2.0 BACKGROUND INFORMATION AND OVERVIEW

191 This section provides a conceptual description of ICESat-2's ice-sheet height measurements and
192 gives a brief description of the derived products.

193 2.1 Background

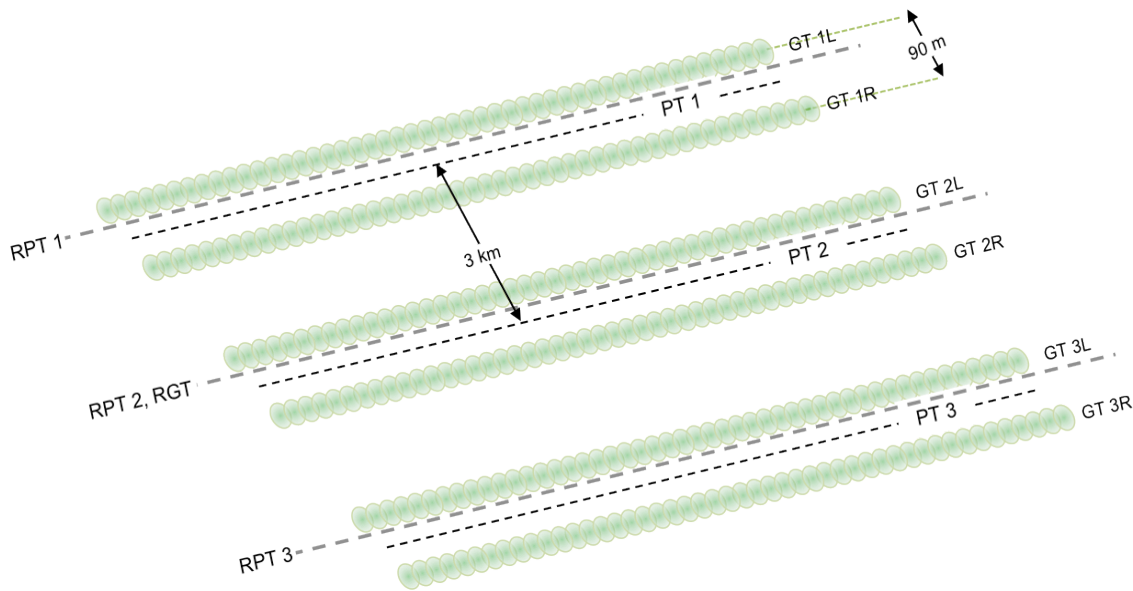
194 The primary goal of the ICESat-2 mission is to estimate mass-balance rates for the Earth's ice
195 sheets. An important step in this process is the calculation of height change at specific locations
196 on the ice sheets. In an ideal world, a satellite altimeter would exactly measure the same point
197 on the earth on each cycle of its orbit. However, there are limitations in a spacecraft's ability to
198 exactly repeat the same orbit and to point to the same location. These capabilities are greatly
199 improving with technological advances but still have limits that need to be accounted for when
200 estimating precise elevation changes from satellite altimetry data. The first ICESat mission
201 allowed estimates of longer-term elevation rates using along-track differencing, because
202 ICESat's relatively precise (50-150-m) pointing accuracy, precise (4-15 m) geolocation
203 accuracy, and small (35-70-m) footprints allowed it to resolve small-scale ice-sheet topography.
204 However, because ICESat had a single-beam instrument, its repeat-track measurements were
205 reliable only for measuring the mean rate of elevation change, because shorter-term height
206 differences could be influenced by the horizontal dispersion of tracks on a sloping surface.

207 ICESat-2 makes repeat measurements over a set of 1387 reference ground tracks (RGTs),
208 completing a *cycle* over all of these tracks every 91 days. ICESat-2's ATLAS instrument
209 employs a split-beam design, where each laser pulse is divided six separate beams. The beams
210 are organized into three *beam pairs*, with each separated from its neighbors by 3.3 km (**Figure**
211 **2-1**), each pair following a reference pair track (RPT) that is parallel to the RGT. The beams
212 within each pair separated by 90 m, which means that each cycle's measurement over an RPT
213 can determine the surface slope independently, and a height difference can be derived from
214 any two measurements of an RPT. The 90-m spacing between the laser beams in each pair
215 is equal to twice the required RMS accuracy with which ICESat-2 can be pointed at its RPTs,
216 which means that for most, but not all, repeat measurements of a given RPT, the pairs of
217 beams will overlap one another. To obtain a record of elevation change from the collection
218 of paired measurements on each RPT, some correction is still necessary to account for the
219 effects of small-scale surface topography around the RPT in the ATL06 surface heights that
220 appear as a result of this non-exact pointing. ATL11 uses a polynomial fit to the ATL06
221 measurements to correct for small-scale topography effects on surface heights that result
222 from this non-exact pointing.

223 The accuracy of ICESat-2 measurements depends on the thickness of clouds between the
224 satellite and the surface, on the reflectance, slope, and roughness of the surface, and on
225 background noise rate which, in turn, depends on the intensity of solar illumination of the
226 surface and the surface reflectance. It also varies from laser beam to beam, because in each
227 of ICESat-2's beam pairs one beam (the "strong beam") has approximately four times the
228 signal strength of the other (the "weak beam"). Parameters on the ATL06 product allow
229 estimation of errors in each measurement, and allow filtering of most measurements with

230 large errors due to misidentification of clouds or noise as surface returns (blunders), but to
 231 enable higher precision surface change estimates, ATL11 implements further self-
 232 consistency checks that further reduce the effects of errors and blunders.
 233

Figure 2-1. ICESat-2 repeat-track schematic



Schematic drawing showing the pattern made by ATLAS’s 6-beam configuration on the ground, for a track running from lower left to upper right. The 6 beams are grouped into 3 beam pairs with a separation between beams within a pair of 90m and a separation between beam pairs of 3.3 km. The RPTs (Reference Pair Tracks, heavily dashed lines in gray) are defined in advance of launch; the central RPT follows the RGT (Reference Ground Track, matching the nadir track of the predicted orbit). The Ground Tracks are the tracks actually measured by ATLAS (GT1L, GT1R, etc., shown by green footprints). Measured Pair Tracks (PTs, smaller dashed lines in black) are defined by the centers of the pairs of GTs, and deviate slightly from the RPTs because of inaccuracies in repeat-track pointing. The separation of GTs in each pair in this figure is greatly exaggerated relative to the separation of the PTs.

234 **2.2 Elevation-correction Coordinate Systems**

235 We perform ATL11 calculations using the along-track coordinate system described in the
 236 ATL06 ATBD (Smith and others, 2019b, Smith and others, 2019a). The along-track coordinate
 237 is measured parallel to the RGT, starting at each RGT’s origin at the equator. The across-track
 238 coordinate is measured to the left of the RGT, so that the two horizontal basis vectors and the
 239 local vertical vector form a right-handed coordinate system.

240 **2.3 Terminology:**

241 Some of the terms that we will use in describing the ATL11 fitting process and the data
242 contributing are:

243 *RPT*: Reference pair track

244 *Cycle*: ICESat-2 has 1387 distinct reference ground tracks, which its orbit covers every 91 days.
245 One repeat measurement of these reference ground tracks constitutes a cycle.

246 *ATL06 segment*: A 40-meter segment fit to a collection of ATL03 photon-event data, as
247 described in the ATL06 ATBD

248 *ATL06 pair*: Two ATL06 segments from the same cycle with the same *segment_id*. By
249 construction, both segments in the ATL06 pair have the same along-track coordinate, and are
250 separated by the beam-to-beam spacing (approximately 90 m) in the across-track direction

251 *ATL11 RPT point*: The expected location of each ATL11 point on the RPT, equivalent to the
252 beginning of every third geosegment on the RPT, or the center of every third ATL06 segment.

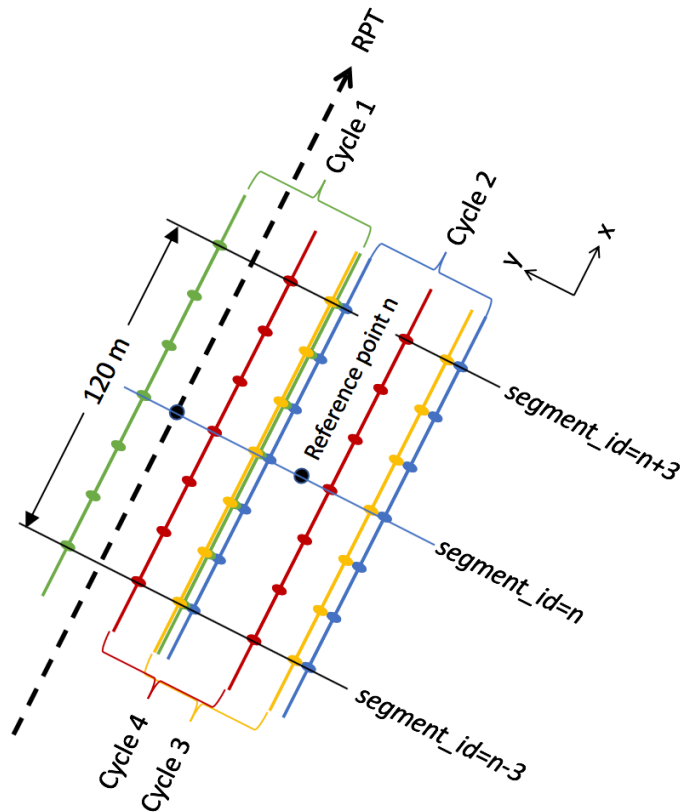
253 *ATL11 reference point*: an *ATL11 RPT point* shifted in the across-track direction to better match
254 the geometry of the available ATL06 data.

255 *ATL11 fit*: The data and parameters associated with a single ATL11 reference point. This
256 includes corrected heights from all available cycles

257

258 ATL11 calculates elevations and elevation differences based on collections of segments from the
259 same beam pair but from different cycles. ATL11 is posted every 60 m, which corresponds to
260 every third ATL06 *segment_id*, and includes ATL06 segments spanning three segments before
261 and after the central segment, so that the ATL11 uses data that span 120 m in the along-track
262 direction. ATL11 data are centered on *reference points*, which has the same along-track
263 coordinate as its central ATL06 segment, but is displaced in the across-track direction to better
264 match the locations of the ATL06 measurements from all of the cycles present (see section
265 3.1.3).

Figure 2-2. ATL06 data for an ATL11 reference point



Schematic of ATL06 data for an ATL11 reference point centered on segment n , based on data from four cycles. The segment centers span 120 m in the along-track data, and the cycles are randomly displaced from the RPT in the across-track direction. The reference point has an along-track location that matches that of segment n , and an across-track position chosen to match the displacements of the cycles.

266

267 2.4 Repeat and non-repeat cycles in the ICESat-2 mission

268 In the early part of the ICESat-2 mission, an error in the configuration of the start trackers
 269 prevented the instrument from pointing precisely at the RGTs. As a result, all data from cycles 1
 270 and 2 were measured between one and two kilometers away from the RGTs, with offsets that
 271 varied in time and as a function of latitude. The measurements from cycles 1 and 2 still give
 272 high-precision measurements of surface height, but repeat-track measurements from ICESat-2
 273 begin during cycle 3, in April of 2019. ATL11 files will be generated for ATL06 granules from
 274 cycles 1 and 2, but these will contain only one cycle of data, plus crossovers, because the
 275 measurements from these cycles (which are displaced from the RPTs by several kilometers) will
 276 not be repeated. We expect the measurements from cycles 1 and 2 to be useful as a reduced-
 277 resolution (compared to ATL06) mapping of the ice sheet, which may prove useful in DEM
 278 generation and in comparisons with other altimetry missions. For cycles 3 and after, each

279 ATL11 granule will contain all available cycles for each RGT (i.e. from cycle 3 onwards), and
280 will contain crossovers between the repeat cycles and cycles 1 and 2.

281 Outside the polar regions, ICESat-2 is pointed to minimize gaps between repeat measurements,
282 and so does not make repeat measurements over its ground tracks. ATL11 is only calculated
283 within the repeat-pointing mask (see Figure ???), which covers areas poleward of 60°N and
284 60°S.

285

286 **2.5 Physical Basis of Measurements / Summary of Processing**

287 Surface slopes on the Antarctic and Greenland ice sheets are generally small, with magnitudes
288 less than two degrees over 99% of Antarctica’s area. Smaller-scale (0.5-3 km) undulations,
289 generated by ice flow over hilly or mountainous terrain may have amplitudes of up to a few
290 degrees. Although we expect that the surface height will change over time, slopes and locations
291 of these smaller-scale undulation are likely controlled by underlying topography and should
292 remain essentially constant over periods of time comparable with the expected 3-7 duration of
293 the ICESat-2 mission. This allows us to use estimates of ice-sheet surface shape derived from
294 data spanning the full mission to correct for small (<130-m) differences in measurement
295 locations between repeat measurements of the same RPT, to produce records of height change
296 for specific locations. To account for changes in the ice-sheet surface slope associated with
297 gradients in thinning, we also solve for the rate of surface-slope change, when sufficient data are
298 available. Further, we can use the surface slope estimates in ATL06 to determine whether
299 different sets of measurements for the same fit center are self-consistent: We can assume that if
300 an ATL06 segment shows a slope significantly different from others measured near the same
301 reference point it likely is in error. The combination of parameters from ATL06 and these self-
302 consistency checks allows us to generate time series based on the highest-quality measurements
303 for each reference point, and our reference surface calculation lets us correct for small-scale
304 topography and to estimate error magnitudes in the corrected data.

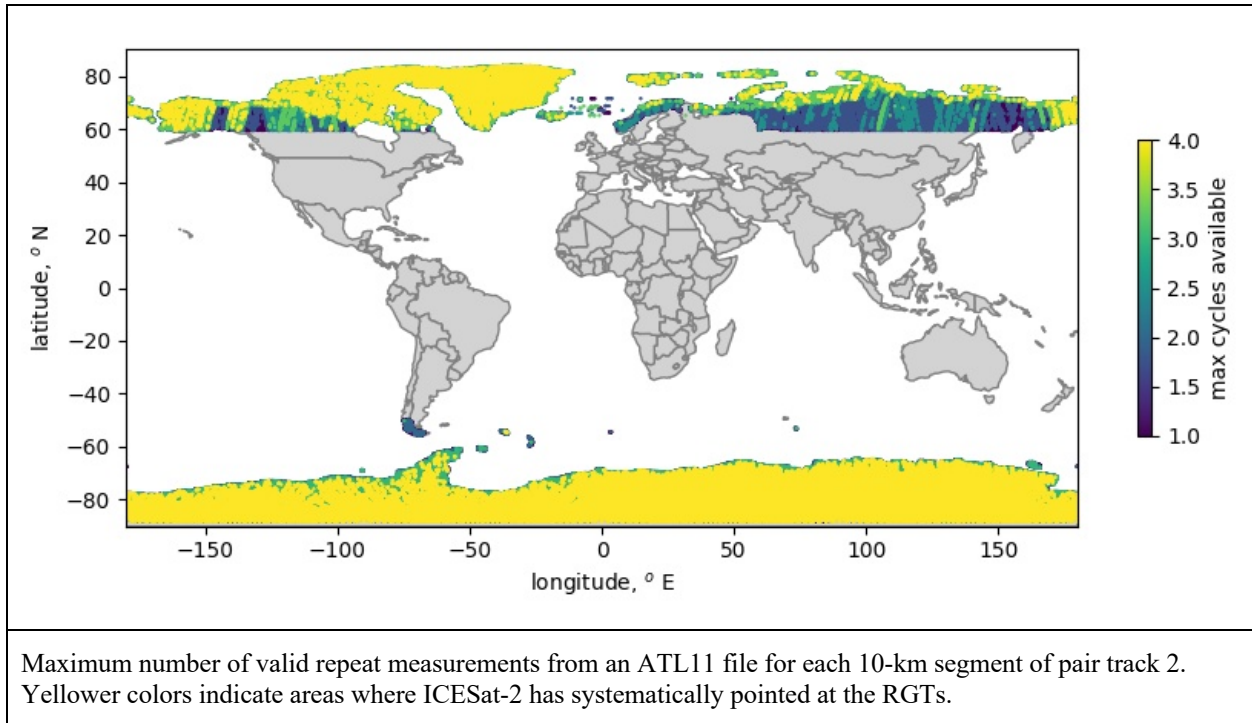
305 **2.5.1 Choices of product dimensions**

306 We have chosen a set of dimensions for the ATL11 fitting process with the goal of creating a
307 product that is conveniently sized for analysis of elevation changes, while still capturing the
308 details of elevation change in outlet glaciers. The assumption that ice-sheet surface can be
309 approximated by a low-degree polynomial becomes untenable as data from larger and larger
310 areas are included in the calculation; therefore we use data from the smallest feasible area to
311 define our reference surface, while still including enough data to reduce the sampling error in the
312 data and to allow for the possibility that at least one or two will encounter a flat surface, which
313 greatly improves the chances that each cycle will be able to measure surface comparable to one
314 another. Each ATL11 point uses data from an area up to 120 m in the along-track direction by
315 up to 130 m in the across-track direction. We have chosen the cross-track search distance
316 ($L_{\text{search_XT}}$) to be 65 m, approximately equal to half the beam spacing, plus three times the
317 observed 6.5 m standard deviation of the across-track pointing accuracy for cycles 3 and 4 in
318 Antarctica. We chose the across-track search distance ($L_{\text{search_AT}}$) to be 60 m, approximately

319 equal to $L_{\text{search_XT}}$, so that the full $L_{\text{search_AT}}$ search window spans three ATL06 segments before
 320 and after the central segment for each reference point. The resulting along-track resolution is
 321 around one third that of ATL06, but still allows 6-7 distinct elevation-change samples across a
 322 small (1-km) outlet glacier.

323 **2.6 Product coverage**

Figure 2-3. Potential ATL11 coverage



324 Over the vegetated parts of the Earth, ICESat-2 makes spatially dense measurements, measuring
 325 tracks parallel to the reference tracks in a strategy that will eventually measure global vegetation
 326 with a track-to-track spacing better than 1 km. Because ATL11 relies upon repeat measurements
 327 over reference tracks to allow the calculation of its reference surfaces, ATL11 is generated for
 328 ICESat-2 subregions 3-5 and 10-12 (global coverage, north and south of 60 degrees). Repeat
 329 measurements are limited to Antarctica, Greenland, and the High Arctic islands (Figure 2-3),
 330 although in other areas the fill-in strategy developed for vegetation measurements allows some
 331 repeat measurements. In regions where ICESat-2 was not pointed to the repeat track, most
 332 ATL11 reference points will provide one measurement close to the RPT. Crossover data are
 333 available for many of these points, though their distribution in time is not regular. A future
 334 update to the product may provide crossover measurements for lower-latitude areas, but the
 335 current product format is not designed to allow this.

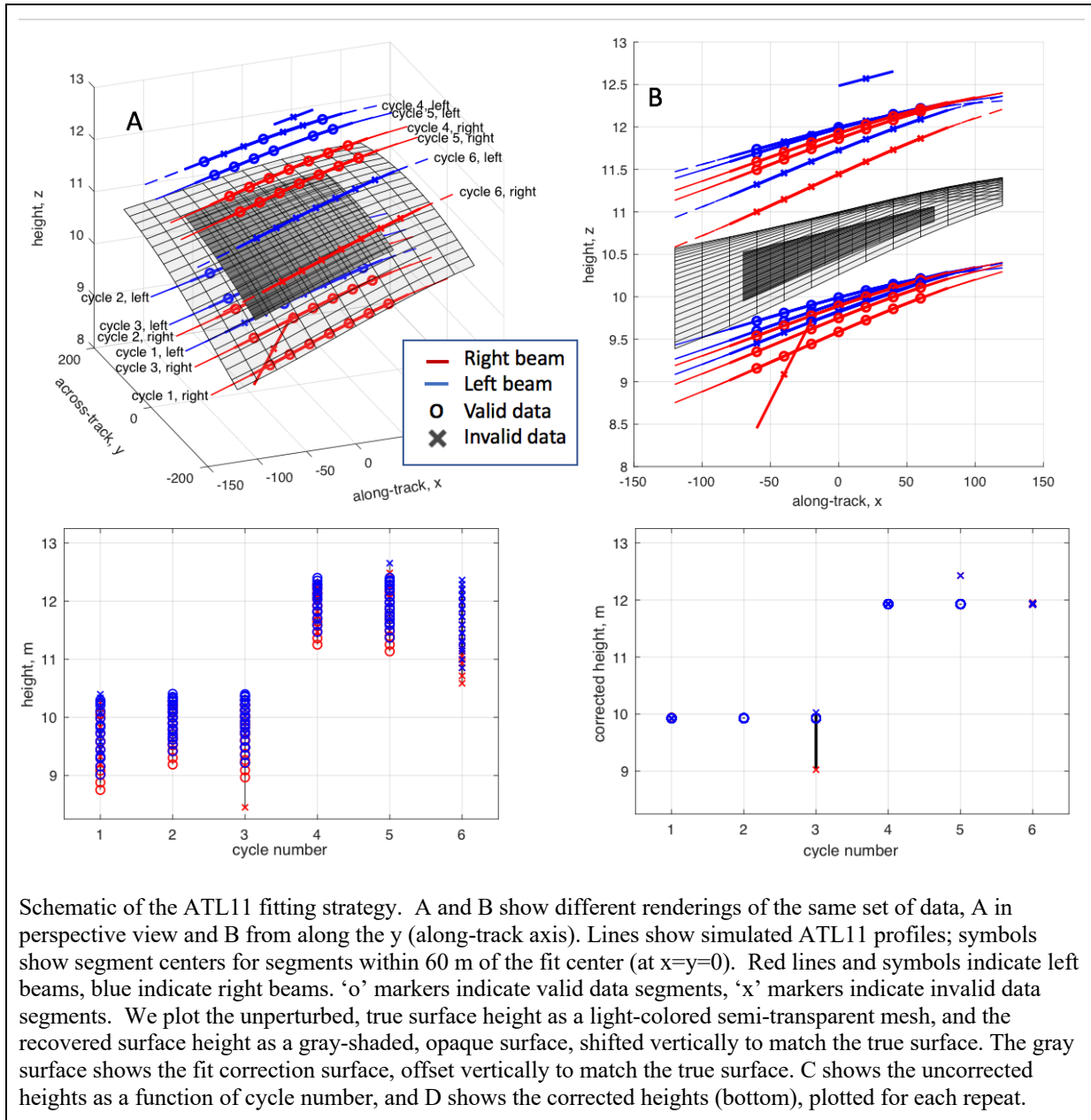
336 **3.0 ALGORITHM THEORY: DERIVATION OF LAND ICE H (T)/ATL11 (L3B)**

337 In this section, we describe in detail the algorithms used in calculating the ATL11 land-ice
338 parameters. This product is intended to provide time series of surface heights for land-ice and
339 ice-shelf locations where ICESat-2 operates in repeat-track mode (*i.e.* for polar ice), along with
340 parameters useful in determining whether each height estimate is valid or a result of a variety of
341 potential errors (see ATL06 ATBD, section 1).

342 ATL11 height estimates are generated by correcting ATL06 height measurements for the
343 combined effects of short-scale (40-120-m) surface topography around the fit centers and small
344 (up to 130-m) horizontal offsets between repeat measurements. We fit a polynomial reference
345 surface to height measurements from different cycles as a function of horizontal coordinates
346 around the fit centers, and use this polynomial surface to correct the height measurements to the
347 fit center. The resulting values reflect the time history of surface heights at the reference points,
348 with minimal contributions from small-scale local topography.

349 In this algorithm, for a set of reference points spaced every 60 meters along each RPT (centered
350 on every third segment center), we consider all ATL06 segments with centers within 60 m along-
351 track and 65 m across-track of the reference point, so that each ATL11 fit contains as many as
352 seven distinct along-track segments from each laser beam and cycle. We select a subset of these
353 segments with consistent ATL06 slope estimates and small error estimates, and use these
354 segments to define a time-variable surface height and a polynomial surface-shape model. We
355 then use the surface-shape model to calculate corrected heights for the segments from cycles not
356 included in the initial subset. We propagate errors for each of these steps to give formal errors
357 estimates that take into account the sampling error from ATL06, and propagate the geolocation
358 errors with the slope of the surface-shape model to give an estimate of systematic errors in the
359 height estimates.

Figure 3-1. ATL11 fitting schematic



Schematic of the ATL11 fitting strategy. A and B show different renderings of the same set of data, A in perspective view and B from along the y (along-track axis). Lines show simulated ATL11 profiles; symbols show segment centers for segments within 60 m of the fit center (at $x=y=0$). Red lines and symbols indicate left beams, blue indicate right beams. 'o' markers indicate valid data segments, 'x' markers indicate invalid data segments. We plot the unperturbed, true surface height as a light-colored semi-transparent mesh, and the recovered surface height as a gray-shaded, opaque surface, shifted vertically to match the true surface. The gray surface shows the fit correction surface, offset vertically to match the true surface. C shows the uncorrected heights as a function of cycle number, and D shows the corrected heights (bottom), plotted for each repeat.

360

361 Figure 3-1 shows a schematic diagram of the fitting process. In this example, we show simulated
 362 ATL06 height measurements for six 91-day orbital cycles over a smooth ice-sheet surface
 363 (transparent grid). Between cycles 3 and 4, the surface height has risen by 2 m. Two of the
 364 segments contain errors: The weak beam for one segment from repeat 3 is displaced downward
 365 and has an abnormal apparent slope in the x direction, and one segment from repeat 5 is
 366 displaced upwards, so that its pair has an abnormal apparent slope in the y direction. Segments
 367 falling within the across and along-track windows of the reference point (at $x=y=0$ in this plot)
 368 are selected, and fit with a polynomial reference surface (shown in gray). When plotted as a

369 function of cycle number (panel C), the measured heights show considerable scatter but when
 370 corrected to the reference surface (panel D), each cycle shows a consistent height, and the
 371 segments with errors are clearly distinct from the accurate measurements.

372 **3.1 Input data editing**

373 Each ATL06 measurement includes location estimates, along- and across-track slope estimates,
 374 and PE (Photon-Event)-height misfit estimates. To calculate the reference surface using the most
 375 reliable subset of available data, we perform tests on the surface-slope estimates and error
 376 statistics from each ATL06-pair to select a self-consistent set of data. These tests determine
 377 whether each pair of measurements is *valid* and can be used in the reference-shape calculation or
 378 is *invalid*. Segments from invalid pairs may be used in elevation-change calculations, but not in
 379 the reference-shape calculation.

380 A complete flow chart of the data-selection process is shown in Figure 3-2, and the parameters
 381 used to make these selections and their values are listed in Table 3-1.

382

383 **Table 3-1 Parameter Filters to determine the validity of segments for ATL11 estimates**

complex_surface_flag	Segment parameter	Filter strategy	Section
0	<i>ATL06_quality_summary</i>	<i>ATL06_quality_summary</i> =0 (indicates high-quality segments)	3.1.1
1	<i>SNR_significance</i>	<i>SNR_significance</i> < 0.02 (indicates low probability of surface-detection blunders)	3.1.1
0 or 1	Along-track differences	Minimum height difference between the endpoints of a segment and the middles of its neighbors must be < 2 m (for smooth surfaces) or < 10 m (for complex surfaces)	3.1.1
0 or 1	<i>h_li_sigma</i>	<i>h_li_sigma</i> < max(0.05, 3*median(<i>h_li_sigma</i>))	3.1.1
0 or 1	Along-track slope	<i>r_slope_x</i> < 3 <i>slope_tolerance_x</i>	3.1.2
0 or 1	Across-track slope	<i>r_slope_y</i> < 3 <i>slope_tolerance_y</i>	3.1.2

398 1) For smooth ice-sheet surfaces, we use the ATL06 *ATL06_quality_summary* parameter,
 399 combined with a measure of along-track elevation consistency, *at_min_dh*, that is calculated as
 400 part of ATL11. *ATL06_quality_summary* is based on the spread of the residuals for each
 401 segment, the along-track surface slope, the estimated error, and the signal strength. Zero values
 402 indicate that no error has been found. We define the along-track consistency parameter
 403 *at_min_dh* as the minimum absolute difference between the heights of the endpoints of each
 404 segment and the center heights of the previous and subsequent segments. Its value will be small
 405 if a segment's height and slope are consistent with at least one of its neighbors. For smooth
 406 surfaces, we require that the *at_min_dh* values be less than 2 m. Over smooth ice-sheet surfaces,
 407 the 2-m threshold eliminates most blunders without eliminating a substantial number of high-
 408 quality data points.

409 2) For rough, crevassed surfaces, the smooth-ice strategy may not identify a sufficient number of
 410 pairs for ATL11 processing to continue. If fewer than one third of the original cycles remain
 411 after the smooth-surface criteria are applied, we relax our criteria, using the signal-to-noise ratio
 412 (based on the ATL06 *segment_stats/snr_significance* parameter) to select the pairs to include in
 413 the fit, and require that the *at_min_dh* values be less than 10 m. If we relax the criteria in this
 414 way, we mark the reference point as having a complex surface using the
 415 *ref_surf/complex_surface_flag*, which limits the degree of the polynomial used in the reference
 416 surface fitting to 0 or 1 in each direction.

417 For either smooth or rough surfaces, we perform an additional check using the magnitude of
 418 *h_li_sigma* for each segment. If any segment's value is larger than three times the maximum of
 419 0.05 m and the median *h_li_sigma* for the valid segments for the current reference point, it is
 420 marked as invalid. The limiting 0.05 m value prevents this test from removing high-quality data
 421 over smooth ice-sheet surfaces, where errors are usually small.

422 Each of these tests applies to values associated with ATL06 segments. When the tests are
 423 complete, we check each ATL06 pair (*i.e.* two segments for the same along-track location from
 424 the same cycle) and if either of its two segments has been marked as invalid, the entire pair is
 425 marked as invalid.

426 3.1.2 Input data editing by slope

427 The segments selected in 3.1.1 may include some high-quality segments and some lower-quality
 428 segments that were not successfully eliminated by the data-editing criteria. We expect that the
 429 ATL06 slope fields (*dh_fit_dx*, and *dh_fit_dy*) for the higher-quality data should reflect the
 430 shape of an ice-sheet surface with a spatially consistent surface slope around each reference
 431 point, but that at least some of lower-quality data should have slope fields that outliers relative to
 432 this consistent surface slope. In this step, we assume that the slope may vary linearly in *x* and *y*,
 433 and so use residuals between the slope values and a regression of the slope values against *x* and *y*
 434 to identify the data with inconsistent slope values. The data with large residuals are marked as
 435 *invalid*.

436 Starting with valid pairs from 3.2.1, we first perform a linear regression between the *y* slopes of
 437 the pairs and the pair-center *x* and *y* positions. The residuals to this regression define one
 438 *y_slope_residual* for each pair. We compare these residuals against a *y_slope_tolerance*:

$$y_slope_tolerance = \max(0.01, 3 \text{ median } (dh_fit_dy_sigma), 3 \text{ RDE } (y_slope_residuals)) \quad 1$$

439 Here RDE is the Robust Difference Estimator, equal to half the difference between the 16th and
 440 84th percentiles of a distribution, and the minimum value of 0.01 ensures that this test does not
 441 remove high-quality segments in regions where the residuals are very consistent. If any pairs
 442 have a *y_slope_residual* greater than *y_slope_tolerance*, we remove them from the group of valid
 443 pairs, then repeat the regression, recalculate *y_slope_tolerance*, and retest the remaining pairs.

444 We then return to the pairs marked as *valid* from 3.1.1, and perform a linear regression between
 445 the *x* slopes of the segments within the pairs and the segment-center *x* and *y* positions. The
 446 residuals to this regression define one *x_slope_residual* for each segment. We compare these
 447 residuals against an *x_slope_tolerance*, calculated in the same way as (1), except using segment *x*
 448 slopes and residuals instead of pair *y* slopes. As with the *y* regression, we repeat this procedure
 449 once if any segments are eliminated in the first round.

450 After both the *x* and *y* regression procedures are complete, each pair of segments is marked as
 451 *valid* if both of its *x* residuals are smaller than *slope_tolerance_x* and its *y* residual is smaller than
 452 *slope_tolerance_y*.

453 3.1.3 Spatial data editing

454 The data included in the reference-surface fit fall in a “window” defined by a $2L_{search\ XT}$ by
 455 $2L_{search\ AT}$ rectangle, centered on each reference point. Because the across-track location of the
 456 repeat measurements for each reference point are determined by the errors in the repeat track
 457 pointing of ATLAS, a data selection window centered on the RPT in the *y* direction will not
 458 necessarily capture all of the available cycles of data. To improve the overlap between the
 459 window and the data, we shift the reference point in the *y* direction so that the window includes
 460 as many valid beam pairs as possible. We make this selection after the parameter-based (3.1.1)
 461 and slope-based (3.1.2) editing steps because we want to maximize the number high-quality pairs
 462 included, without letting the locations of low-quality segments influence our choice of the
 463 reference-point shift.

464 We select the across-track offset for each reference point by searching a range of offset values, δ ,
 465 around the RPT to maximize the following metric:

$$M(\delta) = \frac{[\text{number of unique valid pairs entirely contained in } \delta \pm L_{search\ XT}] + [\text{number of unpaired segments contained in } \delta \pm L_{search\ XT}]/100}{2} \quad 2$$

466 Maximizing this metric allows the maximum number of pairs with two valid segments to be
 467 included in the fit, while also maximizing the number of segments included close to the center of
 468 the fit. If multiple values of δ have the same *M* value we choose the median of those δ values.
 469 The across-track coordinate of the adjusted reference point is then $y_0 + \delta_{max}$, where y_0 is the
 470 across-track coordinate of the unperturbed reference point. After this adjustment, the segments

471 in pairs that are contained entirely in the across-track interval $\delta \pm L_{search\ XT}$ are identified as
 472 *valid* based on the spatial search.

473 The location of the adjusted reference point is reported in the data group for each pair track, with
 474 corresponding local coordinates in the *ref_surf* subgroup: */ptx/ref_surf/x_atc*, */ptx/ref_surf/y_atc*.

475

476 3.2 Reference-Surface Shape Correction

477 To calculate the reference-surface shape correction, we construct the background surface shape
 478 from valid segments selected during 3.1 and 3.2, using a least-squares inversion that separates
 479 surface-shape information from elevation-change information. This produces surface shape-
 480 corrected height estimates for cycles containing at least one valid pair, and a surface-shape
 481 model that we use in later steps (3.4, 3.6) to calculate corrected heights for cycles that contain no
 482 valid pairs and to calculate corrected heights for crossing tracks.

483 3.2.1 Reference-surface shape inversion

484 The reference-shape inversion solves for a reference surface and a set of corrected-height values
 485 that represent the time-varying surface height at the reference point. The inversion involves
 486 three matrices:

487 (i): a polynomial surface shape matrix, **S**, that describes the functional basis for the spatial part of
 488 the inversion:

$$\mathbf{S} = \left[\left(\frac{x - x_0}{l_0} \right)^p \left(\frac{y - y_0}{l_0} \right)^q \right] \quad 3$$

489 Here x_0 and y_0 are equal to the along-track coordinates of the adjusted reference point,
 490 */ptx/ref_surf/x_atc* and */ptx/ref_surf/y_atc*, respectively. **S** has one column for each permutation
 491 of p and q between zero and the degree of the surface polynomial in each dimension, but does
 492 not include a $p=q=0$ term. The degree is chosen to be no more than 3 (in the along-track
 493 direction) or 2 (in the across-track direction), and to be no more than the number of distinct pair-
 494 center y values (in the across-track direction) or more than 1 less than the number of distinct x
 495 values (in the along-track direction) in any cycle, with distinct values defined at a resolution of
 496 20 m in each direction. The scaling factor, l_0 , ensures that the components of **S** are on the order
 497 of 1, which improves the numerical accuracy of the computation. We set $l_0=100$ m, to
 498 approximately match the intra-pair beam spacing.

499 (ii): a matrix that encodes the repeat structure of the data, that accounts for the height-change
 500 component of the inversion:

$$\mathbf{D} = [\delta(i, 1), \delta(i, 2), \dots, \delta(i, N)] \quad 4$$

501 Here δ is the delta function, equal to 1 when its arguments are equal, zero otherwise, and i is an
 502 index that increments by one for each distinct cycle in the selected data.

503 (iii): a matrix that describes the linear rate of change in the surface slope over the course of the
504 mission:

$$\mathbf{S}_t = \left[\left(\frac{x - x_0}{l_0} \right) \left(\frac{t - t_0}{\tau} \right), \left(\frac{y - y_0}{l_0} \right) \left(\frac{t - t_0}{\tau} \right) \right] \quad 5$$

505 Here t_0 is equal to *slope_change_t0*, the mid-point of the mission at the time that ATL11 is
506 generated, halfway between start repeat track pointing (the beginning of cycle 3) and either the
507 end of the mission or the processing time (*slope_change_t0* is an attribute of each ATL11
508 file). This implies that on average, $(t - t_0)$ will have a zero mean. The time-scaling factor, τ , is
509 equal to one year (86400*365.25 seconds). This component will only be included in ATL11
510 once eight complete cycles of data are available on the RGTs (after cycle 10 of the mission).

511 The surface shape, slope change, and height time series are estimated by forming a composite
512 design matrix, \mathbf{G} , where

$$\mathbf{G} = [\mathbf{S} \ \mathbf{S}_t \ \mathbf{D}], \quad 6$$

513 and a covariance matrix, \mathbf{C} , containing the squares of the segment-height error estimates on its
514 diagonal. The surface-shape polynomial and the height changes are found:

$$[\mathbf{s}, \mathbf{s}_t, \mathbf{z}_c] = \mathbf{G}^{-g} \mathbf{z}$$

where

$$\mathbf{G}^{-g} = [\mathbf{G}^T \mathbf{C}^{-1} \mathbf{G}]^{-1} \mathbf{G}^T \mathbf{C}^{-1} \quad 7$$

515 The notation $[\]^{-1}$ designates the inverse of the quantity in brackets, and \mathbf{z} is the vector of segment
516 heights. The parameters derived in this fit are \mathbf{s} , a vector of surface-shape polynomial
517 coefficients, \mathbf{s}_t , the mean rate of surface-slope change, and \mathbf{z}_c , a vector of corrected height values,
518 giving the height at (lat_0, lon_0) as inferred from the height measurements and the surface
519 polynomial. The matrix \mathbf{G}^{-g} is the generalized inverse of \mathbf{G} . The values of \mathbf{s} are reported in the
520 *ref_surf/poly_ref_surf* parameter, as they are calculated from (6), with no correction made for the
521 scaling in (3). The values for the slope-change rates are reported in *ref_surf/slope_change_rate*,
522 after rescaling to units of *years⁻¹*.

523 3.2.2 Misfit analysis and iterative editing

524 If blunders remain in the data input to the reference-surface calculation, they can lead to
525 inaccurate reference surfaces. To help remove these blunders, we iterate the inversion procedure
526 in 3.2.1, eliminating outlying data points based on their residuals to the reference surface.

527 To determine whether outliers may be present, we calculate the chi-squared misfit between the
528 data and the fit surface based on the data covariance matrix and the residual vector, r :

$$\chi^2 = r^T \mathbf{C}^{-1} r \quad 8$$

529 To determine whether this misfit statistic indicates consistency between the polynomial surface
 530 and the data we use a P statistic, which gives the probability that the given χ^2 value would be
 531 obtained from a random Gaussian distribution of data points with a covariance matrix \mathbf{C} . If the
 532 probability is less than 0.025, we perform some further filtering/editing: we calculate the RDE of
 533 the scaled residuals, eliminate any pairs containing a segment whose scaled residual magnitude is
 534 larger than three times that value, and repeat the remaining segments.

535 After each iteration, any column of \mathbf{G} that has a uniform value (i.e. all the values are the same) is
 536 eliminated from the calculation, and the corresponding value of the left-hand side of equation 7
 537 is set to zero. Likewise, if the inverse problem has become less than overdetermined (i.e., the
 538 number of data is smaller than the number of unknown values they are constraining), the
 539 polynomial columns of \mathbf{G} are eliminated one by one until the number of data is greater than the
 540 number of unknowns. Columns are eliminated in descending order of the sum of x and y
 541 degrees, and when there is a tie between columns based on this criterion, the column with the
 542 larger y degree is eliminated first.

543 This fitting procedure is continued until no further segments are eliminated. If more than three
 544 complete cycles that passed the initial editing steps are eliminated in this way, the surface is
 545 assumed to be too complex for a simple polynomial approximation, and we proceed as follows:

546 (i) the fit and its statistics are reported based on the complete set of pairs that passed
 547 the initial editing steps (valid pairs), using a planar ($x_degree = y_degree = 1$) fit in x and y .

548 (ii) the *ref_surf/complex_surface_flag* is set to 1.

549 The misfit parameters are reported in the *ref_surf* group: The final chi-squared statistic is
 550 reported as *ref_surf/misfit_chi2r*, equal to the chi-squared statistic divided by the number of
 551 degrees of freedom in the solution; the final RMS of the scaled residuals is reported as
 552 *ref_surf/misfit_rms*.

553 3.3 Reference-shape Correction Error Estimates

554 We first calculate the errors in the corrected surface heights for segments included in the
 555 reference-surface fit. We form a second covariance matrix, \mathbf{C}_1 , whose diagonal elements are the
 556 maximum of the squares of the segment errors and $\langle r^2 \rangle$. We estimate the covariance matrix for
 557 the height estimates:

$$\mathbf{C}_m = \mathbf{G}^{-g} \mathbf{C}_1 \mathbf{G}^{-gT} \quad 9$$

558 The square roots of the diagonal values of \mathbf{C}_m give the estimated errors in the surface-polynomial
 559 and height estimates due to short-spatial-scale errors in the segment heights. If there are N_{coeff}
 560 coefficients in the surface-shape polynomial, and $N_{shape-cycles}$ cycles included in the surface-shape
 561 fit, then the first N_{coeff} diagonal elements of \mathbf{C}_m give the square of the errors in the surface-shape
 562 polynomial and the last $N_{shape-cycles}$ give the errors in the surface heights for the cycles included in
 563 the fit. The portion of \mathbf{C}_m that refers only to the surface shape and surface-shape change
 564 components is $\mathbf{C}_{m,s}$.

565 **3.4 Calculating corrected height values for repeats with no selected pairs**

566 Once the surface polynomial has been established from the edited data set, corrected heights are
 567 calculated for the unselected cycles (*i.e.* those from which all pairs were removed in the editing
 568 steps): For the segments among these cycles, we form a new surface and slope-change design
 569 matrix, $[\mathbf{S}, \mathbf{S}_t]$ and multiply it by $[\mathbf{s}, \mathbf{s}_t]$ to give the surface-shape correction:

$$\mathbf{z}_c = \mathbf{z} - [\mathbf{S}, \mathbf{S}_t][\mathbf{s}, \mathbf{s}_t] \quad 10$$

570 Here \mathbf{s} is the surface-shape polynomial, and \mathbf{s}_t is the slope-change-rate estimate. This gives up to
 571 fourteen corrected-height values per unselected cycle. From among these, we select the segment
 572 with the minimum error, as calculated in the next step.

573 The height errors for segments from cycles not included in the surface-shape fit are calculated:

$$\sigma_{z,c}^2 = \text{diag}([\mathbf{S}, \mathbf{S}_t]\mathbf{C}_{m,s}[\mathbf{S}, \mathbf{S}_t]^T) + \sigma_z^2 \quad 11$$

574 Here σ_z is the error in the segment height, and $\sigma_{z,c}$ is the error in the corrected height. The
 575 results of these calculations give a height and a height error for each unselected segment. To
 576 obtain a corrected elevation for each repeat that contains no selected pairs, we identify the
 577 segment from that repeat that has the smallest error estimate, and report the value z_c as that
 578 repeat's *ptx/h_corr*, and use $\sigma_{z,c}$ as its error (*ptx/h_corr_sigma*).

579 **3.5 Calculating systematic error estimates**

580 The errors that have been calculated up to this point are due to errors in fitting segments to
 581 photon-counting data and due to inaccuracies in the polynomial fitting model. Additional error
 582 components can result from more systematic errors, such as errors in the position of ICESat-2 as
 583 derived from POD, and pointing errors from PPD. These are estimated in the ATL06
 584 *sigma_geo_xt*, *sigma_geo_at*, and *sigma_geo_r* parameters, and their average for each repeat is
 585 reported in the *cycle_stats* group under the same parameter names. The geolocation component
 586 of the total height is the product of the geolocation error and the surface slope, added in
 587 quadrature with the vertical height error:

$$\sigma_{h,systematic} = \left[\left(\frac{dh}{dx} \sigma_{geo,AT} \right)^2 + \left(\frac{dh}{dy} \sigma_{geo,XT} \right)^2 + \sigma_{geo,r}^2 \right]^{1/2} \quad 12$$

588 For selected segments, which generally come from pairs containing two high-quality height
 589 estimates, dh/dy is estimated from the ATL06 *dh_fit_dy* parameter. For unselected segments, it is
 590 based on the y component of the reference-surface slope, as calculated in section 4.2.

591 The error for a single segment's corrected height is:

$$\sigma_{h,total} = [\sigma_{h,systematic}^2 + \sigma_{h,c}^2]^{1/2} \quad 13$$

592 This represents the total error in the surface height for a single corrected height. In most cases,
 593 error estimates for averages of ice-sheet quantities will depend on errors from many segments
 594 from different reference points, and the spatial scale of the different error components will need
 595 to be taken into account in error propagation models. To allow users to separate these effects,
 596 we report both the uncorrelated error, */ptx/h_corr_sigma*, and the component due only to
 597 systematic errors, */ptx/h_corr_sigma_systematic*. The total error is the quadratic sum of the two,
 598 as described in equation 13.

599 3.6 Calculating shape-corrected heights for crossing-track data

600 Locations where groundtracks cross provide opportunities to check the accuracy of
 601 measurements by comparing surface-height estimates between the groundtracks, and also offers
 602 the opportunity to generate elevation-change time series that have more temporal detail than the
 603 91-day repeat cycle can offer for repeat-track measurements.

604 At these crossover points, we use the reference surface calculated in 3.5 to calculate corrected
 605 elevations for the crossing tracks. We refer to the track for which we have calculated the
 606 reference surface as the *datum* track, and the other track as the *crossing* track. To calculate
 607 corrected surface heights for the crossing ICESat-2 orbits, we first select all data from the
 608 crossing orbit within a distance *L_search_XT* of the updated reference point on the datum track.
 609 For most datum reference points, this will yield no crossing data, in which case the calculation
 610 for that datum point terminates. If crossing data are found, we then calculate the coordinates of
 611 these points in the reference point's along-track and across-track coordinates. This calculation
 612 begins by transforming the crossing-track data into local northing and easting coordinates
 613 relative to the datum reference-point location:

$$\delta N_c = \frac{\pi R_e}{180} (lat_c - lat_d) \quad 14$$

$$\delta E_c = \frac{\pi R_e}{180} (lon_c - lon_d) \cos(lat_c)$$

614 Here (lat_d, lon_d) are the coordinates of the adjusted datum reference point, (lat_c, lon_c) are the
 615 coordinates of the points on the crossing track, and R_e is the local radius of the WGS84 ellipsoid.
 616 We then convert the northing and easting coordinates into along-track and across-track
 617 coordinates based on the azimuth ϕ of the datum track:

$$\begin{aligned} x_c &= \delta N_c \cos(\phi) + \delta E_c \sin(\phi) \\ y_c &= \delta N_c \sin(\phi) - \delta E_c \cos(\phi) \end{aligned} \quad 15$$

618 Using these coordinates, we proceed as we did in 3.4 and 3.5: we generate S_k and S_{kt} matrices,
 619 use them to correct the data and to identify the data point with the smallest error for each
 620 crossing cycle. We report the time, error estimate, and corrected height for the minimum-error
 621 datapoint from each cycle, as well as the location, pair, and track number corresponding to the
 622 datum point in the */ptx/crossing_track_data* group. Because the crossing angles between the
 623 tracks are oblique at high latitudes, a particular crossing track may appear in a few subsequent
 624 datum points; in these cases, we expect that the error estimates should vary with the distance

625 between the crossing track and the datum track, so that the point with the minimum error should
 626 correspond to the precise crossing location of the two tracks.

627 To help evaluate the quality of crossing-track data we calculate the *along_track_rss* parameter
 628 for each crossing-track measurement. This parameter gives the RSS of the differences between
 629 each segment's endpoint heights and the heights of the previous and subsequent segments. A
 630 segment that is consistent with the previous and next segments in slope and elevation will have a
 631 small value for this parameter, a segment that is inconsistent (and thus potentially in error) will
 632 have a large value. Crossing-track measurements that have values greater than 10 m are
 633 excluded from ATL11 and do not appear in the dataset.

634 3.7 Calculating parameter averages

635 ATL11 contains a variety of parameters that mirror parameters in ATL06, but are averaged to the
 636 140-m ATL11 resolution. Except where noted otherwise, these quantities are weighted averages
 637 of the corresponding ATL06 values. For selected pairs (i.e. those included in the reference-
 638 surface fit), the parameters are averaged over the selected segments from each cycle, using
 639 weights derived from their formal errors, *h_li_sigma*. The parameter weighted average for the N_k
 640 segments from cycle k is then:

$$\langle q \rangle = \frac{\sum_{i=1}^{N_k} |\sigma_i^{-2}| q_i}{\sum_{i=1}^{N_k} |\sigma_i^{-2}|} \quad 16$$

641 Here q_i are the parameter values for the segments. For repeats with no selected pairs, recall that
 642 the corrected height for only one segment is reported in */ptx/h_corr*; for these, we simply report
 643 the corresponding parameter values for that selected segment.

644

645 3.8 Output data editing

646 The output data product includes cycle height estimates only for those cycles that have
 647 non-systematic error estimates (*/ptx/h_corr_sigma*) less than 15 m. All other heights (and their
 648 errors) are reported as *invalid*.

649

650

651 4.0 LAND ICE PRODUCTS: LAND ICE H (T)(ATL 11/L3B)

652 Each ATL11 file contains data for a single reference ground track, for one of the subregions
 653 defined for ATLAS granules (see Figure 6-3). The ATL11 consists of three top-level groups, one
 654 for each beam pair (*pt1*, *pt2*, *pt3*). Within each pair-track group, there are datasets that give the
 655 corrected heights for each cycle, their errors, and the reference-point locations. Subgroups
 656 (*cycle_stats*, and *ref_surf*) provide a set of data-quality parameters, and ancillary data describing
 657 the fitting process, and use the same ordering and coordinates as the top-level group (i.e. any
 658 dataset within the */ptx/cycle_stats* and */ptx/ref_surf* groups refers to the same latitude, longitude,
 659 and reference points as the corresponding measurements in the */ptx/* groups.) The
 660 *crossing_track_data* group gives height measurements at crossover locations, and has its own set
 661 of locations and
 662

663 4.1.1 File naming convention

664 ATL11 files are named in the following format:

665 `ATL11_ttttgg_cccc_rrr_vv.h5`

666 Here *tttt* is the rgt number, *gg* is the granule-region number, *cccc* gives the first and last cycles of
 667 along-track data included in the file (e.g. `_0308_` would indicate that cycles three through eight,
 668 inclusive, might be included in the along-track solution), and *rrr* is the release number. and *vv* is
 669 the version number, which is set to one the first time a granule is generated for a given data
 670 release, and is incremented by one if the granule is regenerated.

671

672 4.2 */ptx* group

673 4.3

674 shows the datasets in the *ptx* groups. This group gives the principal output parameters of the
 675 ATL11. The corrected repeat measurements are in */ptx/h_corr*, which gives improved height
 676 measurements based on a surface fit to valid data at paired segments. The associated reference
 677 coordinates, */ptx/latitude* and */ptx/longitude* give the reference point location, with averaged
 678 times per repeat, */ptx/delta_time*. For repeats with no selected pairs, the corrected height is that
 679 from the selected segment with the lowest error. Two error metrics are given in
 680 */ptx/h_corr_sigma* and */ptx/h_corr_sigma_systematic*. The first gives the error component due to
 681 ATL06 range errors and due to uncertainty in the reference surface. The second gives the
 682 component due to geolocation and radial-orbit errors that are correlated at scales larger than one
 683 reference point; adding these values in quadrature gives the total per-cycle error. Values are only
 684 reported for */ptx/h_corr*, */ptx/h_corr_sigma*, and */ptx/h_corr_sigma_systematic* for those cycles
 685 whose uncorrelated errors are less than 15 m; all others are reported as *invalid*. A
 686 */ptx/quality_summary* is included for each cycle, based on fit statistics from ATL06.

687

688

Table 4-1 Parameters in the /ptx/ group

Parameter	Units	Dimensions	Description
<i>cycle_number</i>	counts	$I \times N_{cycles}$	Cycle number for each column of the data
<i>latitude</i>	degrees North	$N_{pts} \times I$	Reference point latitude
<i>longitude</i>	degrees East	$N_{pts} \times I$	Reference point longitude
<i>ref_pt</i>	counts	$N_{pts} \times I$	The reference point number, <i>m</i> , counted from the equator crossing of the RGT.
<i>delta_time</i>	seconds	$N_{pts} \times N_{cycles}$	mean GPS time for the segments for each cycle
<i>h_corr</i>	meters	$N_{pts} \times N_{cycles}$	the mean corrected height
<i>h_corr_sigma</i>	meters	$N_{pts} \times N_{cycles}$	the formal error in the corrected height
<i>h_corr_sigma_systematic</i>	meters	$N_{pts} \times N_{cycles}$	the magnitude of the RSS of all errors that might be correlated at scales larger than a single reference point (e.g. pointing errors, GPS errors, etc)
<i>quality_summary</i>	counts	$N_{pts} \times N_{cycles}$	summary flag: zero indicates high-quality cycles: where $\min(\text{signal_selection_source}) \leq 1$ and $\min(\text{SNR_significance}) < 0.02$, and $\text{ATL06_summary_zero_count} > 0$.

689

690 4.4 /ptx/ref_surf group

691 Table 4-2 describes the /ptx/ref_surf group. This group includes parameters describing the
 692 reference surface fit at each reference point. The polynomial coefficients are given in
 693 /ptx/poly_ref_surf, sorted first by total degree, then by x-component degree. Because the
 694 polynomial degree is chosen separately for each reference point, enough columns are provided in
 695 the /ptx/poly_ref_surf and /ptx/poly_ref_surf_sigma to accommodate all possible components up
 696 to 2rd degree in y and 3th degree in x, and absent values are filled in with zeros. The
 697 correspondence between the columns of the polynomial fields and the exponents of the x and y
 698 terms are given in the /ptx/poly_exponent_x and /ptx/poly_exponent_y fields. The time origin for
 699 the slope change is given in the group attribute /ptx/slope_change_t0.

Table 4-2 Parameters in the /ptx/ref_surf group

Parameter	Units	Dimensions	Description
<i>complex_surface_flag</i>	counts	$N_{pts} \times I$	0 indicates that normal fitting was attempted, 1 indicates that the signal selection algorithm rejected too many repeats, and only a linear fit was attempted
<i>rms_slope_fit</i>	counts	$N_{pts} \times I$	the RMS of the slope of the fit polynomial within 50 m of the reference point
<i>e_slope</i>	counts	$N_{pts} \times I$	the mean East-component slope for the reference surface within 50 m of the reference point
<i>n_slope</i>	counts	$N_{pts} \times I$	the mean North-component slope for the reference surface within 50 m of the reference point
<i>at_slope</i>	Counts	$N_{pts} \times I$	Mean along-track component of the slope of the reference surface within 50 m of the reference point
<i>xt_slope</i>		$N_{pts} \times I$	Mean across-track component of the slope of the reference surface within 50 m of the reference point
<i>deg_x</i>	counts	$N_{pts} \times I$	Maximum degree of non-zero polynomial components in x
<i>deg_y</i>	counts	$N_{pts} \times I$	Maximum degree of non-zero polynomial components in y

<i>poly_exponent_x</i>	counts	1×8	Exponents for the x factors in the surface polynomial
<i>poly_exponent_y</i>	counts	1×8	Exponents for the y factors in the surface polynomial
<i>poly_coeffs</i>	counts	$N_{pts} \times 8$	polynomial coefficients (up to degree 3), for polynomial components scaled by 100 m
<i>poly_ref_coeffs_sigma</i>	counts	$N_{pts} \times 8$	formal errors for the polynomial coefficients
<i>ref_pt_number</i>	counts	$N_{pts} \times 1$	Ref point number, counted from the equator crossing along the RGT.
<i>x_atc</i>	meters	$N_{pts} \times 1$	Along-track coordinate of the reference point, measured along the RGT from its first equator crossing.
<i>y_atc</i>	meters	$N_{pts} \times 1$	Across-track coordinate of the reference point, measured along the RGT from its first equator crossing.
<i>rgt_azimuth</i>	degrees	$N_{pts} \times 1$	Reference track azimuth, in degrees east of local north
<i>slope_change_rate_x</i>	years ⁻¹	$N_{pts} \times 1$	rate of change of the x component of the surface slope
<i>slope_change_rate_y</i>	years ⁻¹	$N_{pts} \times 1$	rate of change of the y component of the surface slope
<i>slope_change_rate_x_sigma</i>	years ⁻¹	$N_{pts} \times 1$	Formal error in the rate of change of the x component of the surface slope
<i>slope_change_rate_y_sigma</i>	years ⁻¹	$N_{pts} \times 1$	Formal error in the rate of change of the y component of the surface slope
<i>misfit_chi2r</i>	meters	$N_{pts} \times 1$	misfit chi square, divided by the number of degrees in the solution
<i>misfit_rms</i>	meters	$N_{pts} \times 1$	RMS misfit for the surface-polynomial fit
<i>fit_quality</i>	counts	$N_{pts} \times 1$	Indicates quality of the fit:

			<p>0: no problem identified</p> <p>1: One or more polynomial coefficient errors larger than 2</p> <p>2: One or more components of the surface slope has magnitude larger than 0.2</p> <p>3: Conditions 1 and 2 both true.</p>
--	--	--	---

700
701

702 The slope of the fit surface is given in the *ref_surf/n_slope* and *ref_surf/e_slope* parameters in
703 the local north and east directions; the corresponding slopes in the along-track and across-track
704 directions are given in the *ref_surf/xt_slope* and *ref_surf/yt_slope* parameters. For the along-
705 track points, the surface slope is calculated by evaluating the correction-surface polynomial for a
706 10-m spaced grid of points extending ± 50 m in *x* and *y* around the reference point, and
707 calculating the mean slopes of these points. The calculation is performed in along-track
708 coordinates and then projected onto the local north and east vectors. The *rms_slope_fit*
709 derived from the same set of points, and is calculated as the RMS of the standard deviations of
710 the slopes calculated from adjacent grid points, in *x* and *y*.

711

712 **4.5 /ptx/cycle_stats group**

713 The */ptx/cycle_stats* group gives summary information about the segments present for each
714 reference point. Most parameters are averaged according to equation 14, but for others (e.g.
715 */ptx/signal_selection_flag_best*, which is the minimum of the signal selection flags for the cycle)
716 **Table 4-3** describes how the summary statistics are derived.

717

718 **Table 4-3 Parameters in the /ptx/cycle_stats group**

Parameter	Units	Dimensions	Description
<i>ATL06_summary_zero_count</i>	counts	$N_{pts} \times N_{cycles}$	Number of segments with <i>atl06_quality_summary</i> =0 (0 indicates the best-quality data)
<i>h_rms_misfit</i>	meters	$N_{pts} \times N_{cycles}$	Weighted-average RMS misfit between PE heights and along-track land-ice segment fit
<i>r_eff</i>	counts	$N_{pts} \times N_{cycles}$	Weighted-average effective, uncorrected reflectance for each cycle.

Parameter	Units	Dimensions	Description
<i>tide_ocean</i>	meters	$N_{pts} \times N_{cycles}$	Weighted-average ocean tide for each cycle
<i>dac</i>	meters	$N_{pts} \times N_{cycles}$	Dynamic atmosphere correction (mainly the effect of atmospheric pressure on floating-ice elevation).
<i>cloud_flg_atm</i>	counts	$N_{pts} \times N_{cycles}$	Minimum cloud flag from ATL06: Flag indicates confidence that clouds with $OT^* > 0.2$ are present in the lower 3 km of the atmosphere based on ATL09
<i>cloud_flg_asr</i>	counts	$N_{pts} \times N_{cycles}$	Minimum apparent-surface-reflectance - based cloud flag from ATL06: Flag indicates confidence that clouds with $OT > 0.2$ are present in the lower 3 km of the atmosphere based on ATL09
<i>bsnow_h</i>	meters	$N_{pts} \times N_{cycles}$	Weighted-average blowing snow layer height for each cycle
<i>bsnow_conf</i>	counts	$N_{pts} \times N_{cycles}$	Maximum <i>bsnow_conf</i> flag from ATL06: indicates the greatest (among segments) confidence flag for presence of blowing snow for each cycle
<i>x_atc</i>	meters	$N_{pts} \times N_{cycles}$	weighted average of pair-center RGT y coordinates for each cycle
<i>y_atc</i>	meters	$N_{pts} \times N_{cycles}$	weighted mean of pair-center RGT y coordinates for each cycle
<i>ref_pt</i>		$N_{pts} \times N_{cycles}$	Ref point number, counted from the equator crossing along the RGT.
<i>seg_count</i>	counts	$N_{pts} \times N_{cycles}$	Number of segments marked as valid for each cycle. Equal to 0 for those cycles not included in the reference-surface shape fit.
<i>min_signal_selection_source</i>	counts	$N_{pts} \times N_{cycles}$	Minimum of the ATL06 <i>signal_selection_source</i> value (indicates the highest-quality segment in the cycle)
<i>min_snr_significance</i>	counts	$N_{pts} \times N_{cycles}$	Minimum of <i>SNR_significance</i> (indicates the quality of the best segment in the cycle)

Parameter	Units	Dimensions	Description
<i>sigma_geo_h</i>	meters	$N_{pts} \times N_{cycles}$	Root-mean-weighted-square-average total vertical geolocation error due to PPD and POD
<i>sigma_geo_at</i>	meters	$N_{pts} \times N_{cycles}$	Root-mean-weighted-square-average local-coordinate x horizontal geolocation error for each cycle due to PPD and POD
<i>sigma_geo_xt</i>	meters	$N_{pts} \times N_{cycles}$	Root-mean-weighted-square-average local-coordinate y horizontal geolocation error for each cycle due to PPD and POD
<i>h_mean</i>	meters	$N_{pts} \times N_{cycles}$	Weighted-average of surface heights, not including the correction for the reference surface

719 *OT (optical thickness) is a measure of signal attenuation used in atmospheric calculations. This
 720 parameter discussed in ICESat-2 atmospheric products (ATL09)

721

722 **4.6 /ptx/crossing_track_data group**

723 The /ptx/crossing_track_data group (Table 4-4) contains elevation data at crossover locations.
 724 These are locations where two ICESat-2 pair tracks cross, so data are available from both the
 725 datum track, for which the granule was generated, and from the crossing track. The data in this
 726 group represent the elevations and times from the crossing tracks, corrected using the reference
 727 surface from the datum track. Each set of values gives the data from a single segment on the
 728 crossing track, that was selected as having the minimum error among all segments on the
 729 crossing track within the $2 L_{search_XT}$ –by- $2 L_{search_AT}$ window around the reference point
 730 on the datum track. The systematic errors are evaluated based on the magnitude of the reference-
 731 surface slope and the magnitude of the horizontal geolocation error of the crossing-track data.
 732 Attributes for the group specify the track number and pair-track number of the crossing track.

733

Table 4-4 Parameters in the /ptx/crossing_track_data group

Parameter	Units	Dimensions	Description
<i>ref_pt</i>	counts	$N_{XO} \times 1$	the reference-point number for the datum track
<i>delta_time</i>	years	$N_{XO} \times 1$	time relative to the ICESat-2 reference epoch

<i>h_corr</i>	meters	$N_{XO} \times 1$	WGS-84 height, corrected for the ATL11 surface shape
<i>h_corr_sigma</i>	meters	$N_{XO} \times 1$	error in the height estimate
<i>h_corr_sigma_systematic</i>	meters	$N_{XO} \times 1$	systematic error in the height estimate
<i>ocean_tide</i>	Meters	$N_{XO} \times 1$	Ocean-tide estimate for the crossing track
<i>dac</i>	Meters	$N_{XO} \times 1$	Dynamic atmosphere correction for the crossing track
<i>latitude</i>	degrees	$N_{XO} \times 1$	latitude of the crossover point
<i>longitude</i>	degrees	$N_{XO} \times 1$	longitude of the crossover point
<i>cycle_number</i>	counts	$N_{XO} \times 1$	Cycle number for the crossing data
<i>rgt</i>	counts	$N_{XO} \times 1$	The RGT number for the crossing data
<i>spot_crossing</i>	counts	$N_{XO} \times 1$	The spot number for the crossing data
<i>atl06_quality_summary</i>	counts	$N_{XO} \times 1$	quality flag for the crossing data derived from ATL06. 0 indicates no problems detected, 1 indicates potential problems
<i>along_track_rss</i>	meters	$N_{XO} \times 1$	Root sum of the squared differences between the heights of the endpoints for the crossing-track segment and the centers of the previous and next segments

734

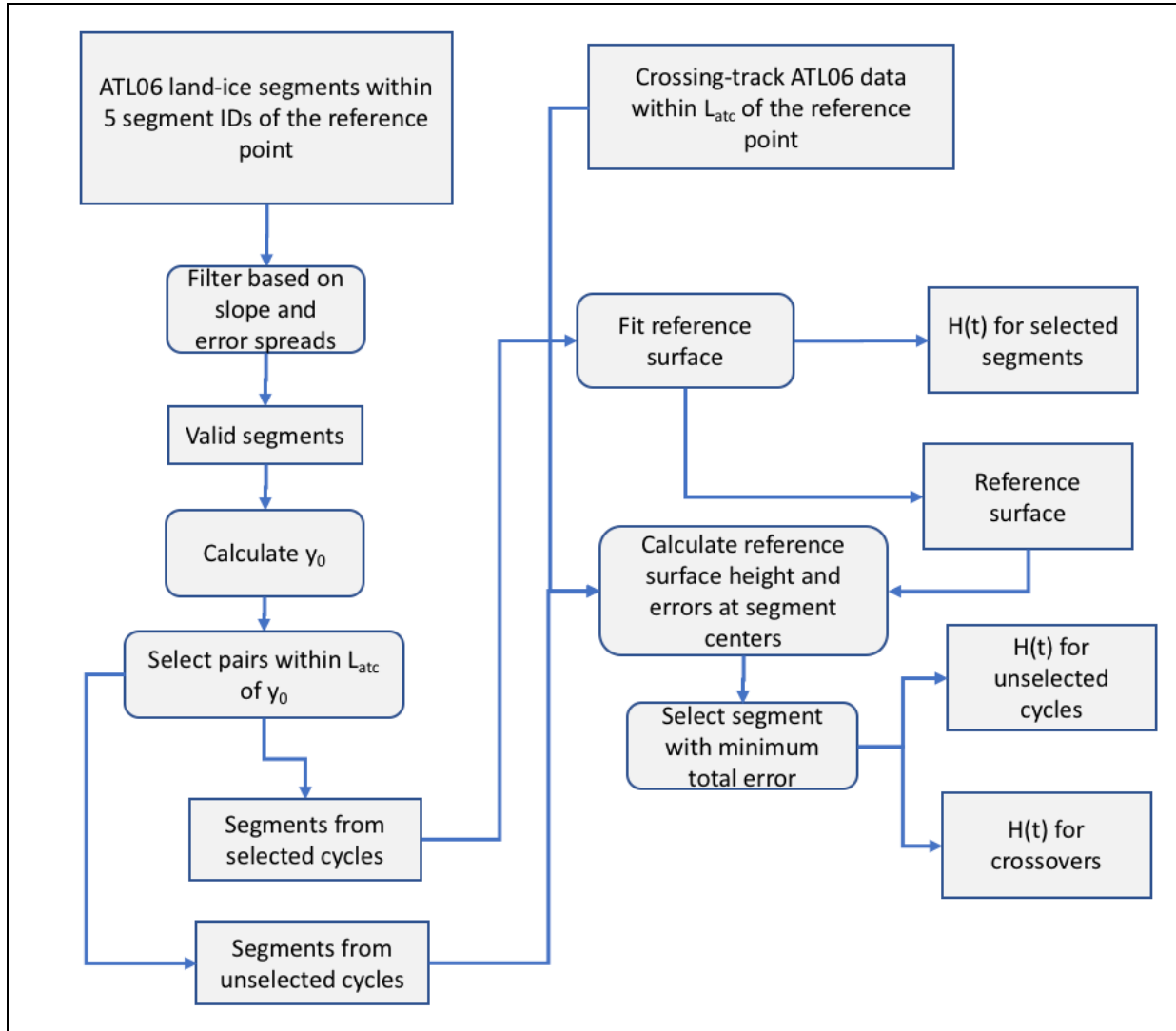
735

736 5.0 ALGORITHM IMPLEMENTATION

737

738

Figure 5-1 Flow Chart for ATL11 Surface-shape Corrections



739

740

741 The following steps are performed for each along-track reference point.

742

743

744

745

746

1. Segments with *segment_id* within $N_search/2$ of the reference-point number, are selected.
2. Valid segments are identified based on estimated errors, the *ATL06_quality_summary* parameter, and the along- and across-track segment slopes. Valid pairs, containing valid measurements from two different beams, are also identified.

- 747 3. The location of the reference point is adjusted to allow the maximum number of repeats
 748 with at least one valid pair to fall within the across-track search distance of the reference
 749 point.
 750 4. The reference surface is fit to pairs with two valid measurements within the search
 751 distance of the reference point. This calculation also produces corrected heights for the
 752 selected pairs and the errors in the correction polynomial coefficients.
 753 5. The correction surface is used to derive corrected heights for segments not selected in
 754 steps 1-3, and the height for the segment with the smallest error is selected for each
 755 6. The reference surface is used to calculate heights for external (pre-ICESat-2) laser
 756 altimetry data sets and crossover ICESat-2 data.

757 A schematic of this calculation is shown in Figure 5-1.

758 5.1.1 Select ATL06 data for the current reference point

759 **Inputs:**

760 *ref_pt*: segment number for the current reference point

761 *track_num*: The track number for current point

762 *pair_num*: The pair number for the current point

763 **Outputs:**

764 *D_ATL06*: ATL06 data structure

765 **Parameters:**

766 *N_search*: number of segments to search, around *ref_pt*, equal to 5.

767 **Algorithm:**

- 768 1. For each along-track point, load all ATL06 data from track *track_num* and pair *pair_num* that
 769 have *segment_id* within *N_search* of *ref_pt*: These segments have $ref_pt - N_search$
 770 $\leq segment_id \leq ref_pt + N_search$.
 771 2. Reject any data that have *y_atc* values more than 500 m distant from the nominal pair-track
 772 centers (3200 m for pair 1, 0 m for pair 2, -3200 m for pair 3).

773

774 5.1.2 Select pairs for the reference-surface calculation

775 **Inputs:**

776 *ref_pt*: reference point number for the current fit

777 *x_atc_ctr*: Along-track coordinate of the reference point

778 *D_ATL06*: ATL06 data structure

779 *pair_data*: Structure describing ATL06 pairs, includes mean of strong/weak beam *y_atc* and

780 *dh_fit_dy*

781 **Outputs:**

782 **validity flags for each segment:**

783 *valid_segs.x_slope*: Segments identified as valid based on x-slope consistency

784 *valid_segs.data*: Segments identified as valid based on ATL06 parameter values.

785 **Validity flags for each pair:**

786 *valid_pairs*: Pairs selected for the reference-surface calculation

787 *valid_pairs.y_slope*: Pairs identified as valid based on y-slope consistency

788 *y_polyfit_ctr*: y center of the slope regression

789 *ref_surf/complex_surface_flag*: Flag indicating 0: non-complex surface, 1: complex surface.

790

791 **Parameters:**

792 *L_search_XT*: The across-track search distance.

793 *N_search*: Along-track segment search distance

794 *seg_sigma_threshold_min*: Minimum threshold for accepting errors in segment heights, equal to
795 0.05 m.

796 **Algorithm:**

797 1. Flag valid segments based on ATL06 values.

798 1a. Count the cycles that contain at least one pair that has *atl06_quality_flag*=0
799 for both segments. If this number is greater than $N_cycles/3$, set
800 *ref_surf/complex_surface_flag*=0 and set *valid_segs.data* to 1 for segments with
801 *ATL06_quality_summary* equal to 0. Otherwise, set *ref_surf/complex_surface_flag*=1 and set
802 *valid_segs.data* to 1 for segments with *snr_significance* < 0.02.

803 1b. Define *seg_sigma_threshold* as the maximum of 0.05 or three times the median of
804 *sigma_h_li* for segments with *valid_segs.data* equal to 1. Set *valid_segs.data* to 1 for segments
805 with *h_sigma_li* less than this threshold and *ATL06_quality_summary* equal to 0.

806 1c. Define *valid_pairs.data*: For each pair of segments, set *valid_pairs.data* to 1 when
807 both segments are marked as valid in *valid_segs.data*.

808 2. Calculate representative values for the *x* and *y* coordinate for each pair, and filter by distance.

809 2a. For each pair containing two defined values, set *pair_data.x* to the segments' *x_atc*
810 value, and *pair_data.y* to the mean of the segments' *y_atc* values.

811 2b. Calculate *y_polyfit_ctr*, equal to the median of *pair_data.y* for pairs marked valid in
812 *valid_pairs.data*.

813 2c. Set *valid_pairs.ysearch* to 1 for pairs with $|pair_data.y - y_polyfit_ctr| <$
814 *L_search_XT*.

- 815 3. Select pairs based on across-track slope consistency
- 816 3a. Define *pairs_valid_for_y_fit*, for the across-track slope regression if they are marked
817 as valid in *valid_pairs.data*, and *valid_pairs.ysearch*, not otherwise.
- 818 3b. Choose the degree of the regression for across-track slope
- 819 -If the valid pairs contain at least two different *x_atc* values (separated by at least
820 18 m), set the along-track degree, *my_regression_y_degree*, to 1, 0 otherwise.
- 821 -If valid pairs contain at least two different *ref_surf/y_atc* values (separated by at
822 least 18 m), set the across-track degree, *my_regression_y_degree*, to 1, 0 otherwise.
- 823 3c. Calculate the formal error in the y slope estimates: *y_slope_sigma* is the RSS of the
824 *h_li_sigma* values for the two beams in the pair divided by the difference in their *y_atc*
825 values. Based on these, calculate *my_regression_tol*, equal to the maximum of 0.01 or three
826 times the median of *y_slope_sigma* for valid pairs (*pairs_valid_for_y_fit*).
- 827 3d. Calculate the regression of *dh_fit_dy* against *pair_data.x* and *pair_data.y* for valid
828 pairs (*pairs_valid_for_y_fit*). The result is *y_slope_model*, which gives the variation of *dh_fit_dy*
829 as a function of *x_atc* and *y_atc*. Calculate *y_slope_resid*, the residuals between the *dh_fit_dy*
830 values and *y_slope_model* for all pairs in *pair_data*.
- 831 3e. Calculate *y_slope_threshold*, equal to the maximum of *my_regression_tol* and three
832 times the RDE of *y_slope_resid* for valid pairs.
- 833 3f. Mark all pairs with $|y_slope_resid| > y_slope_threshold$ as invalid. Re-establish
834 *pairs_valid_for_y_fit* (based on *valid_pairs.data*, *valid_pairs.y_slope* and *valid_pairs.ysearch*).
835 Return to step 3d (allow two iterations total).
- 836 3g. After the second repetition of 3d-f, use the model to mark all pairs with
837 $|y_slope_resid|$ less than *y_slope_threshold* with 1 in *valid_pairs.y_slope*, 0 otherwise.
- 838 4. Select segments based on along-track slope consistency for both segments in the pair
- 839 4a. Define *pairs_valid_for_x_fit*, valid segments for the along-track slope regression:
840 segments are valid if they come from pairs marked as valid in *valid_pairs.data* and
841 *valid_pairs.ysearch*, not otherwise.
- 842 4b. Choose the degree of the regression for along-track slope
- 843 -If valid segments contain at least two different *x_atc* values set the along-track
844 degree, *mx_regression_x_degree*, to 1, 0 otherwise.
- 845 -If valid segments contain at least two different *y_atc* values, set the across-track
846 degree, *mx_regression_y_degree*, to 1, 0 otherwise.
- 847 4c. Calculate along-track slope regression tolerance, *mx_regression_tol*, equal to the
848 maximum of either 0.01 or three times the median of the *dh_fit_dx_sigma* values for the valid
849 pairs.
- 850 4d. Calculate the regression of *dh_fit_dx* against *pair_data.x* and *pair_data.y* for valid
851 segments (*pairs_valid_for_x_fit*). The result is *x_slope_model*, which gives the variation of

852 *dh_fit_dx* as a function of *pair_data.x* and *pair_data.y*. Calculate *x_slope_resid*, the residuals
 853 between the *dh_fit_dx* and *x_slope_resid* for all segments for this reference point, *seg_x_center*
 854 and *y_polyfit_ctr*.

855 4e. Calculate *x_slope_threshold*, equal to the maximum of either *mx_regression_tol* or
 856 three times the RDE of *x_slope_resid* for valid segments.

857 4f. Mark *valid_segs.x_slope* with $|x_slope_resid| > x_slope_threshold$ as invalid. Re-
 858 establish *valid_pairs.x_slope* when both *valid_segs.x_slope* equal 1. Re-establish
 859 *pairs_valid_for_x_fit*. Return to step 4d (allow two iterations total).

860 4g. After the second repetition of 4d-f, mark all segments with $|x_slope_resid|$ less than
 861 *x_slope_threshold* with 1 in *seg_valid_xslope*, 0 otherwise. Define *valid_pairs.x_slope* as 1 for
 862 pairs that contain two segments with *valid_segs.x_slope*=1, 0 otherwise.

863 5. Re-establish *valid_pairs.all*. Set equal to 1 if *valid_pairs.x_slope*, *valid_pairs.y_slope*,
 864 and *valid_pairs.data* are all valid.

865 5a. Identify *unselected_cycle_segs*, as those *D6.cycles* where *valid_pairs.all* are False.

866

867 **5.1.3 Adjust the reference-point y locaction to include the maximum number of** 868 **cycles**

869 **Inputs:**

870 *D_ATL06*: ATL06 structure for the current reference point.

871 *valid_pairs*: Pairs selected based on parameter values and along- and across-track slopes.

872 **Outputs:**

873 *ref_surf/y_atc*: Adjusted fit-point center *y*.

874 *valid_pairs*: validity masks for pairs, updated to include those identified as valid based on the
 875 spatial search around *y_atc_ctr*.

876 **Parameters:**

877 *L_search_XT*: Across-track search length (equal to 110 m)

878 **Algorithm:**

879 1. Define *y0* as the median of the unique integer values of the pair center *y_atc* for all
 880 valid pairs. Set a range of *y* values, *y0_shifts*, as $\text{round}(y0) \pm 100$ meters in 2-meter increments.

881 2. For each value of *y0_shifts* (*y0_shift*), set a counter, *selected_seg_cycle_count*, to the
 882 number of distinct cycles for which both segments of the pair are contained entirely within the *y*
 883 interval $[y0_shift - L_search_XT, y0_shift + L_search_XT]$. Add to this, the number of distinct
 884 cycles represented by unpaired segments contained within that interval, weighted by 0.01. The
 885 sum is called *score*.

886 3. Search for an optimal y-center value (with the most distinct cycles). Set y_{best} to the
 887 value of $y0_shift$ that maximizes $score$. If there are multiple $y0_shift$ values with the same,
 888 maximum $score$, set to the median of the $y0_shift$ values with the maximum $score$.

889 4. Update $valid_pairs$ to include all pairs with y_atc within +/- L_search_XT from
 890 y_atc_ctr .

891 **5.1.4 Calculate the reference surface and corrected heights for selected pairs**

892 **Inputs:**

893 D_ATL06 : ATL06 structure for the current reference point, containing parameters for each
 894 segment:

895 x_atc : along-track coordinate

896 y_atc : across-track coordinate

897 $delta_t$: time for the segment

898 $pair_data$: Structure containing information about ATL06 pairs. Must include:

899 y_atc : Pair-center across-track coordinates

900 $valid_pairs$: Pairs selected based on parameter values and along- and across-track slope.

901 x_atc_ctr : The reference point along-track x coordinate (equal to ref_surf/x_atc).

902 y_atc_ctr : The reference point along-track x coordinate (equal to ref_surf/y_atc)

903 **Outputs:**

904 ref_surf/deg_x : Degree of the reference-surface polynomial in the along-track direction

905 ref_surf/deg_y : Degree of the reference-surface polynomial in the across-track direction

906 $ref_surf/poly_coeffs$: Polynomial coefficients of the reference-surface fit

907 $ref_surf/poly_coeffs_sigma$: Formal error in polynomial coefficients of the reference-surface fit

908 $ref_surf/slope_change_rate_x$: Rate of change of the x component of the surface slope

909 $ref_surf/slope_change_rate_x_sigma$: Formal error in the rate of change of the x component of
 910 the surface slope

911 $ref_surf/slope_change_rate_y$: Rate of change of the y component of the surface slope

912 $ref_surf/slope_change_rate_y_sigma$: Formal error in the rate of change of the y component of
 913 the surface slope

914 r_seg : Segment residuals from the reference-surface model

915 $/ptx/h_corr$: Partially filled-in per-cycle corrected height for cycles used in reference surface

916 $/ptx/h_corr_sigma$: Partially filled-in per-cycle formal error in corrected height for cycles used in
 917 reference surface

918 ref_surf_cycles : A list of cycles used in defining the reference surface

919 *C_m_surf*: Covariance matrix for the reference-polynomial and surface-change model

920 *fit_columns_surf*: Mask identifying which components of the combined reference-polynomial
 921 and surface-change model were included in the fit.

922 *degree_list_x*: The x degrees corresponding to the columns of matrix used in fitting the reference
 923 surface to the data

924 *degree_list_y*: The y degrees corresponding to the columns of matrix used in fitting the reference
 925 surface to the data

926 *selected_segments*: A set of flags indicating which segments were selected by the iterative
 927 fitting process.

928 Partially filled-n per-cycle ATL11 output variables (see table 4-3) for cycles used in reference
 929 surface

930 **Parameters:**

931 *poly_max_degree_AT*: Maximum polynomial degree for the along-track fit, equal to 3.

932 *poly_max_degree_XT*: Maximum polynomial degree for the across-track fit, equal to 2.

933 *slope_change_t0*: Half the duration of the mission (equal to the time of the last-possible
 934 elevation value minus the time of the start of data collection, divided by two).

935 *max_fit_iterations*: Maximum number of iterations for surface fitting, with acceptable residuals,
 936 equal to 20.

937 *xy_scale*: The horizontal scaling value used in polynomial fits, equal to 100 m

938 *t_scale*: The time scale used in polynomial fits, equal to seconds in 1 year.

939 **Algorithm:**

940 1. Build the cycle design matrix: **G_zp** is a matrix that has one column for each distinct
 941 cycle in *selected_pairs* and one row for each segment whose pair is in *selected_pairs*. For each
 942 segment, the corresponding row of **G_zp** is 1 for the column matching the cycle for that segment
 943 and zero otherwise.

944 2. Select the polynomial degree.

945 The degree of the x polynomial, *ref_surf/deg_x*, is:
 946 $\min(\text{poly_max_degree_AT}, \text{maximum}(\text{number of distinct values of } \text{round}((x_atc - x_atc_ctr)/20)$
 947 **among the selected segments in any one cycle**) - 1), and the degree of the y polynomial,
 948 *ref_surf/deg_y*, is : $\min(\text{poly_max_degree_XT}, \text{number of distinct values of}$
 949 $\text{round}((\text{pair_data.y_atc} - \text{y_atc_ctr})/20)$ among the selected pairs)

950 3. Perform an iterative fit for the reference-surface polynomial.

951 3a. Define *degree_list_x* and *degree_list_y*: This array defines the x and y degree of the
 952 polynomial coefficients in the polynomial surface model. There is one component for each
 953 unique degree combination of x degrees between 0 and *ref_surf/deg_x* and for y degree between
 954 0 and *ref_surf/deg_y* such that $x_degree + y_degree \leq \max(\text{ref_surf/deg_x}, \text{ref_surf/deg_y})$,

955 except that there is no $x_degree=0$ and $y_degree=0$ combination. They are sorted first by the
 956 sum of the x and y degrees, then by x degree, then by y degree.

957 3b. Define the polynomial fit matrix. **S_fit_poly** has one column for each element of
 958 the polynomial degree arrays, with values equal to $((x_atc - x_atc_ctr)/xy_scale)^{x_degree} ((y_atc -$
 959 $y_atc_ctr)/xy_scale)^{y_degree}$. There is one row in the matrix for every segment marked as *selected*.

960 3c. If the time span is longer than 1.5 years, define slope-change matrices,
 961 **S_fit_slope_change**. The first column of the matrix gives the rate of slope change in the x
 962 component, equal to $(x_atc - x_atc_ctr)/xy_scale * (\delta_time - slope_change_t0)/t_scale$. The
 963 second column gives the rate of slope change in the y component, equal to $(y_atc -$
 964 $y_atc_ctr)/xy_scale * (\delta_time - slope_change_t0)/t_scale$.

965 3d. Build the surface matrix, **G_surf**, and the combined surface and cycle-height matrix,
 966 **G_surf_zp**: The surface matrix is equal to the horizontal catenation of **S_fit_poly**, and, if
 967 defined, **S_fit_slope_change**. The combined surface and cycle-height matrix, **G_surf_zp**, is
 968 equal to the horizontal catenation of **G_surf** and **G_zp**.

969 3e. Subset the fitting matrix. Subset **G_surf_zp** by row to include only rows
 970 corresponding to selected segments to produce **G** (on the first iteration, all are *selected*). Next,
 971 subset **G** by column, first to eliminate all-zero columns, and second to include only columns that
 972 are linearly independent from one another: calculate the normalized correlation between each
 973 pair of columns in **G**, and if the correlation is equal to unity, eliminate the column with the
 974 higher weighted degree ($poly_wt_sum = x_degree + 1.1 * y_degree$, with the factor of 1.1
 975 chosen to avoid ties). Identify the selected columns in the matrix as *fit_columns*. If more than
 976 three of the original surface-change columns have been eliminated, set the
 977 *ref_surf/complex_surface_flag* to *True*, mark all columns corresponding to polynomial
 978 coefficients of combined x and y degree greater than 1 as *False* in *fit_columns*.

979 3f. Check whether the inverse problem is under- or even-determined: If the number of
 980 *selected_segments* is less than the number of columns of **G**, eliminate remaining columns of **G** in
 981 descending order of *poly_wt_sum* until the number of columns of **G** is less than the number of
 982 *selected_segments*.

983 3g. Generate the data-covariance matrix, **C_d**. The data-covariance matrix is a square
 984 matrix whose diagonal elements are the squares of the *h_li_sigma* values for the selected
 985 segments.

986 3h. Calculate the polynomial fit. Initialize **m_surf_zp**, the reference model, to a vector of
 987 zero values, with one value for each column of **G_surf_zp**. Calculate the generalized inverse
 988 (equation 7), of **G**, **G_g**. If the inversion calculation returns an error, or if any row of **G_g** is all-
 989 zero (indicating some parameters are not linearly independent), report fit failure and return.
 990 Otherwise, multiply **G_g** by the subset of *h_li* corresponding to the selected segment to give **m**,
 991 containing values for the parameters selected in *fit_columns*. Fill in the components of
 992 **m_surf_zp** flagged in *fit_columns* with the values in **m**.

993 3i. Calculate model residuals for all segments, *r_seg*, equal to $h_li - G_surf_dz *$
 994 **m_surf_zp**. The subset of *r_seg* corresponding to *selected* segments is *r_fit*.

995 3j. Calculate the fitting tolerance, r_tol , equal to three times the RDE of the
 996 r_fit/h_li_sigma for all *selected* segments. Calculate the reduced chi-squared value for these
 997 residuals, $ref_surf/misfit_chi2$, equal to $r_fit^T C_d^{-1} r_fit$. Calculate the P value for the misfit,
 998 equal to one minus the CDF of a chi-squared distribution with $m-n$ degrees of freedom for
 999 $ref_surf/misfit_chi2$, where m is the number of rows in \mathbf{G} , and n is the number of columns.

1000 3k. If the P value is less than 0.025 and fewer than $max_fit_iterations$ have taken place,
 1001 mark all segments for which $|r_seg/h_li_sigma| < r_tol$ as *selected*, and return to 3e. Otherwise,
 1002 continue to 3k.

1003 3l. Propagate the errors. Based on the most recent value of $\mathbf{C_d}$, generate a revised data-
 1004 covariance matrix, $\mathbf{C_dp}$, whose diagonal values are the maximum of h_li_sigma and
 1005 $RDE(r_fit)^2$. Calculate the model covariance matrix, $\mathbf{C_m}$ using equation 9. If any of the
 1006 diagonal elements of $\mathbf{C_m}$ are larger than 10^4 , report a fit failure and return. Fill in elements of
 1007 $\mathbf{m_surf_zp}$ that are marked as valid in $fit_columns$ with the square roots of the corresponding
 1008 diagonal elements of $\mathbf{C_m}$. If any of the errors in the polynomial coefficients are larger than 2,
 1009 set $ref_surf/fit_quality=1$.

1010 4. Return a list of cycles used in determining the reference surface in ref_surf_cycles . These
 1011 cycles have columns in \mathbf{G} that contain a valid pair, and for which the steps 3e and 3j did not
 1012 eliminate the degree of freedom. For these cycles, partially fill in the values of $/ptx/h_corr$ and
 1013 $/ptx/h_corr_sigma$, from \mathbf{m} and $\mathbf{m_sigma}$. Similarly, fill in values for
 1014 $/ptx/h_corr_sigma_systematic$ (Equation 12) and $/ptx/delta_time$, as well as all variables in Table
 1015 4-3. Set $/ptx/h_corr$, $/ptx/h_corr_sigma$, $/ptx/h_corr_sigma_systematic$ to NaN for those cycles
 1016 that have uncorrelated error estimates greater than 15 m.

1017 Values from Table 4-2 defining the fitted reference surface are also reported including
 1018 $ref_surf/poly_coeffs$, and $ref_surf/poly_coeffs_sigma$, $ref_surf/slope_change_rate_x$,
 1019 $ref_surf/slope_change_rate_y$, $ref_surf/slope_change_rate_x_sigma$, and
 1020 $ref_surf/slope_change_rate_y_sigma$.

1021 Return $\mathbf{C_m_surf}$, the portion of $\mathbf{C_m}$ corresponding to the polynomial and slope-change
 1022 components of $\mathbf{C_m}$. Return $selected_cols_surf$, the subset of $selected_cols$ corresponding to the
 1023 surface polynomial and slope-change parameters.

1024 Return the reduced chi-square value for the last iteration, $ref_surf/misfit_chi2r$, equal to
 1025 $ref_surf/misfit_chi2/(m-n)$.

1026

1027 **5.1.5 Calculate corrected heights for cycles with no selected pairs.**

1028 **Inputs:**

1029 **$\mathbf{C_m_surf}$:** Covariance matrix for the reference-surface model.

1030 $degree_list_x$, $degree_list_y$: List of x-, y-, degrees for which the reference-surface calculation
 1031 attempted an estimate.

1032 *selected_cols_surf*: Parameters of the combined reference-surface and slope-change model for
 1033 which the inversion returned a value. There should be one value for each row/column of
 1034 **C_m_surf**.

1035 *x_atc_ctr, y_atc_ctr*: Center point for the surface fit (equal to *ref_surf/x_atc, ref_surf/y_atc*)

1036 *selected_segments*: Boolean array indicating segments selected for the reference-surface
 1037 calculation

1038 *valid_segs.x_slope*: Segments identified as valid based on x-slope consistency

1039 *valid_segs.data*: Segments identified as valid based on ATL06 parameter values.

1040 *pair_number*: Pair number for each segment

1041 *h_li*: Land-ice height for each segment

1042 *h_li_sigma*: Formal error in *h_li*.

1043 */ptx/h_corr*: Partially filled-in per-cycle corrected height

1044 */ptx/h_corr_sigma*: Partially filled-in per-cycle corrected height error

1045 *ref_surf/poly_coefs*: Polynomial coefficients from 2-d reference-surface fit

1046 *ref_surf_cycles*: A list of cycles used in defining the reference surface

1047 *ref_surf/slope_change_rate_x, ref_surf/slope_change_rate_y*: Rate of change of the x and y
 1048 components of the surface slope

1049 *ref_surf/N_slope, ref_surf/E_slope*: slope components of reference surface

1050 *sigma_geo_r*: Radial component of the geolocation error for the crossing track

1051 *D_ATL06*: ATL06 data structure

1052 Partially filled-in per-cycle ATL11 output variables (see table 4-3)

1053 **Outputs:**

1054 */ptx/h_corr*: Per-cycle corrected height

1055 */ptx/h_corr_sigma*: Per-cycle corrected height error

1056 *selected_segments*: A set of arrays listing the selected segments for each cycle.

1057 Per-cycle ATL11 output variables (see table 4-3).

1058 **Algorithm:**

1059 1. Identify the segments marked as valid in *valid_segs.data* and *valid_segs.x_slope* that are not
 1060 members of the cycles in *ref_surf_cycles*. Label these as *non_ref_segments*.

1061 2. Build **G_other**, a polynomial-fitting matrix for the *non_ref_segments*. **G_other** will include
 1062 only the polynomial components listed in *degree_list_x* and *degree_list_y*, and (if the mission
 1063 has been going on for at least 1.5 years) the slope-change components. Multiply **G_other** by
 1064 [*ref_surf/poly_coefs, ref_surf/slope_change_rate_x, ref_surf/slope_change_rate_y*] to give
 1065 corrected heights, *z_kc*.

- 1066 3. Take the subset of **G_other** corresponding to the components in *fit_cols_surf* to make
 1067 **G_other_surf**. Propagate the polynomial surface errors and surface-height errors for
 1068 *non_ref_segments* based on **G_other_surf**, **C_m_surf**, and *h_li_sigma* using equation
 1069 11. These errors are *z_kc_sigma*.
- 1070 4. Identify the segments in *non_ref_segments* for each cycle, and, from among these, select the
 1071 one with the smallest *z_kc_sigma*. If, for this cycle, *z_kc_sigma* is less than 15 m, fill in the
 1072 corresponding values of */ptx/h_corr* and */ptx/h_corr_sigma*. For cycles containing no valid
 1073 segments, report invalid data as NaN. Similarly, fill in the variables in Table 4-3, with the value
 1074 from the segment with the smallest *z_kc_sigma*.

1075

1076 **5.1.6 Calculate corrected heights for crossover data points**

1077 **Inputs:**

- 1078 *C_m_surf*: Covariance matrix for the reference surface model.
 1079 *C_m_surf*: Covariance matrix for the reference-surface model.
 1080 *x_atc_ctr, y_atc_ctr*: Center point for the surface fit, in along-track coordinates
 1081 *lat_d, lon_d*: Latitude and longitude for the adjusted datum reference point (from */ptx/latitude,*
 1082 */ptx/longitude*)
 1083 *PT*: Pair track for the surface fit
 1084 *RGT*: RGT for the surface fit
 1085 *ref_surf/rgt_azimuth*: The azimuth of the RGT, relative to local north
 1086 *lat_c, lon_c*: Location for crossover data
 1087 *time_c*: Time for crossover data
 1088 *h_c*: Elevations for crossover data
 1089 *sigma_h_c*: Estimated errors for crossover data

1090 **Outputs:**

- 1091 *ref_pt*: reference point (not for the crossing track) (ben, which one then?)
 1092 *pt*: pair track for the crossing-track points
 1093 *crossing_track_data/rgt*: Reference ground track for the crossing-track point
 1094 *crossing_track_data/delta_time*: time for the crossing-track point
 1095 *crossing_track_data/h_corr*: corrected elevation for the crossing-track points
 1096 *crossing_track_data/h_corr_sigma*: error in the corrected elevation for the crossing_track points
 1097 *crossing_track_data/h_corr_sigma_systematic*: Error component in the corrected elevation due
 1098 to pointing and orbital errors.

1099 *crossing_track_data/along_track_rss:*

1100 **Parameters:**

1101 *L_search_XT:* Across-track search distance

1102 **Algorithm (executed independently for the data from each cycle of the mission):**

1103 1. Project data points into the along-track coordinate system:

1104 1a: Calculate along-track and across-track vectors:

1105 $x_hat = [\cos(ref_surf/rgt_azimuth), \sin(ref_surf/rgt_azimuth)]$

1106 $y_hat = [\sin(ref_surf/rgt_azimuth), -\cos(ref_surf/rgt_azimuth)]$

1107 1b. Calculate the R_earth , the WGS84 radius at lat_d .

1108 1c: Project the crossover data points into a local projection centered on the fit
1109 center:

1110 $N_d = R_earth (lat_c - lat_d)$

1111 $E_d = R_earth \cos(lat_d) (lon_c - lon_d)$

1112 1d: Calculate the x and y coordinates for the data points, relative to the fit-center point:

1113 $dx_c = \langle x_hat, [E_c, N_c] \rangle$

1114 $dy_c = \langle y_hat, [E_c, N_c] \rangle$

1115 Here $\langle \mathbf{a}, \mathbf{b} \rangle$ is the inner (dot) product of \mathbf{a} and \mathbf{b} .

1116 2. Calculate the fitting matrix using equation 6.

1117 3. Calculate the errors at each point using the fitting matrix and C_m , using on equation 11.

1118 4. Select the minimum-error data point and report the values in **Error! Reference source not**
1119 **found..**

1120 5. Calculate the systematic error in the corrected height:

1121 $crossing_track_data/h_sigma_sigma_systematic = (\sigma_geo_r^2 + (N_d$
1122 $ref_surf/n_slope)^2 + (E_d ref_surf/e_slope)^2)^{1/2}$

1123 6. Calculate the along-track RSS for the selected segment. For each selected crossing segment
1124 calculate the endpoint heights (equal to the segment center height plus or minus 20 meters times
1125 the segment's along-track slope), and calculate the RSS of the differences between these heights
1126 and the center heights of the previous and subsequent segments. If this RSS difference is greater
1127 than 10 m for any cycle, do not report any parameters for that segment's cycle.

1128 **5.1.7 Provide error-averaged values for selected ATL06 parameters**

1129 **Inputs:**

1130 *ATL06 data structure:* ATL06 data to be averaged

1131 *Selected_segments:* A set of arrays listing the selected segments for each cycle.

1132 *Parameter_list*: A list of parameters to be averaged

1133 **Outputs:**

1134 *Parameter_averages*: One value for each parameter and each cycle

1135 **Algorithm:**

1136 1. For each cycle, select the values of *h_li_sigma* based on the values within *selected_segments*.
 1137 Calculate a set of weights, w_i , such that the sum of the weights is equal to 1 and each weight is
 1138 proportional to the inverse square of *h_li_sigma*. If only one value is present in
 1139 *selected_segments*, $w_1=1$.

1140 2. For each parameter, multiply the weights for each cycle by the parameter values, report the
 1141 averaged value in *parameter_averages*.

1142 **5.1.8 Provide miscellaneous ATL06 parameters**

1143 **Inputs:**

1144 *ATL06 data structure*: ATL06 data to be averaged

1145 *Selected_segments*: A set of arrays listing the selected segments for each cycle.

1146 **Outputs:**

1147 Weighted-averaged parameter values, with one value per cycle, filled in with NaN for cycles
 1148 with no selected segments

1149 *cycle_stats/h_robust_sprd*

1150 *h_li_rms_mean* (*ben*, I don't see this in the list)

1151 *cycle_stats/r_eff*

1152 *cycle_stats/tide_ocean*

1153 *cycle_stats/dac*

1154 *cycle_stats/bsnow_h*

1155 *cycle_stats/x_atc*

1156 *cycle_stats/y_atc*

1157 *cycle_stats/sigma_geo_h*

1158 *cycle_stats/sigma_geo_at*

1159 *cycle_stats/sigma_geo_xt*

1160 *cycle_stats/h_mean*

1161 Parameter minimum values, with one value per cycle, filled in NaN for cycles with no selected
 1162 segments:

1163 *cycle_stats/cloud_flg_asr*

1164 *cycle_stats/cloud_flg_atm*

1165 *cycle_stats/bsnow_conf*

1166 Other parameters:

1167 *cycle_stats/strong_spot*: The laser beam number for the strong beam in the pair

1168 **Algorithm:**

1169 1. Select the segments for the cycle indicated in *selected_segments* from the
1170 *ATL06_data_structure*.

1171 2: Based on *h_li_sigma*, calculate the segment weights using equation 14.

1172 3. For ATL06 parameters *h_robust_sprd*, *h_li_rms*, *r_eff*, *tide_ocean*, *dac*, *bsnow_h*, *x_atc*,
1173 *y_atc*, *sigma_geo_h*, *sigma_geo_at*, *sigma_geo_xt*, and *h_mean* calculate the weighted average
1174 of the parameter based on the segment weights. The output parameter names are the same as the
1175 input parameter names in the *cycle_stats* group.

1176 4. For ATL06 parameters *cloud_flg_asr* and *cloud_flg_atm* report the best (minimum) value
1177 from among the selected values. For *bsnow_conf* report the maximum value from among the
1178 selected values.

1179 5. For the *cycle_stats/strong_spot* attribute, report the laser beam number for the strong beam in
1180 the pair.

1181

1182 **5.1.9 Characterize the reference surface**

1183 **Inputs:**

1184 *poly_coeffs*: Coefficients of the surface polynomial

1185 *rgt_azimuth*: the azimuth of the reference ground track

1186 **Outputs:**

1187 *ref_surf/n_slope*: the north component of the reference-surface slope

1188 *ref_surf/e_slope*: the east component of the reference-surface slope

1189 *ref_surf/at_slope*: the along-track component of the reference-surface slope

1190 *ref_surf/xt_slope*: the across-track component of the reference-surface slope

1191 *ref_surf/rms_slope_fit*: the rms slope of the reference surface

1192 **Procedure:**

- 1193 1. Calculate the coordinates of a grid of northing and easting offsets around the reference points,
1194 each between -50 m and 50 m in 10-meter increments: dN , dE
- 1195 2. Translate the coordinates into along and across-track coordinates:
- 1196 $dx = \cos(\text{rgt_azimuth}) * dN + \sin(\text{rgt_azimuth}) * dE$
- 1197 $dy = \sin(\text{rgt_azimuth}) * dN - \cos(\text{rgt_azimuth}) * dE$
- 1198 3. Calculate the polynomial surface elevations for the grid points by evaluating the polynomial
1199 surface at dx and dy : z_poly
- 1200 4. Fit a plane to z_poly as a function of dN and dE . The North coefficient of the plane is
1201 ref_surf/n_slope , the east component is ref_surf/e_slope , the RMS misfit of the plane is
1202 ref_surf/rms_slope_fit . If either component of the slope has a magnitude larger than 0.2, add 2 to
1203 $ref_surf/fit_quality$.
- 1204 5. Fit a plane to z_poly as a function of dx and dy . The along-track coefficient of the plane is
1205 ref_surf/at_slope , the across-track component is ref_surf/xt_slope .
- 1206

1207 **6.0 APPENDIX A: GLOSSARY**

1208 This appendix defines terms that are used in ATLAS ATBDs, as derived from a document
1209 circulated to the SDT, written by Tom Neumann. Some naming conventions are borrowed from
1210 **Spots, Channels and Redundancy Assignments** (ICESat-2-ATSYS-TN-0910) by P. Luers.
1211 Some conventions are different than those used by the ATLAS team for the purposes of making
1212 the data processing and interpretation simpler.

1213

1214 **Spots.** The ATLAS instrument creates six spots on the ground, three that are weak and three that
1215 are strong, where strong is defined as approximately four times brighter than weak. These
1216 designations apply to both the laser-illuminated spots and the instrument fields of view. The
1217 spots are numbered as shown in Figure 1. At times, the weak spots are leading (when the
1218 direction of travel is in the ATLAS +x direction) and at times the strong spots are leading.
1219 However, the spot number does not change based on the orientation of ATLAS. The spots are
1220 always numbered with 1L on the far left and 3R on the far right of the pattern. Not: beams,
1221 footprints.

1222

1223 **Laser pulse (pulse for short).** Individual pulses of light emitted from the ATLAS laser are
1224 called laser pulses. As the pulse passes through the ATLAS transmit optics, this single pulse is
1225 split into 6 individual transmit pulses by the diffractive optical element. The 6 pulses travel to
1226 the earth's surface (assuming ATLAS is pointed to the earth's surface). Some attributes of a laser
1227 pulse are the wavelength, pulse shape and duration. Not: transmit pulse, laser shot, laser fire.

1228

1229 **Laser Beam.** The sequential laser pulses emitted from the ATLAS instrument that illuminate
1230 spots on the earth's surface are called laser beams. ATLAS generates 6 laser beams. The laser
1231 beam numbering convention follows the ATLAS instrument convention with strong beams
1232 numbered 1, 3, and 5 and weak beams numbered 2, 4, and 6 as shown in the figures. Not:
1233 beamlet.

1234

1235 **Transmit Pulse.** Individual pulses of light emitted from the ICESat-2 observatory are called
1236 transmit pulses. The ATLAS instrument generates 6 transmit pulses of light from a single laser
1237 pulse. The transmit pulses generate 6 spots where the laser light illuminates the surface of the
1238 earth. Some attributes of a given transmit pulse are the wavelength, the shape, and the energy.
1239 Some attributes of the 6 transmit pulses may be different. Not: laser fire, shot, laser shot, laser
1240 pulse.

1241

1242 **Reflected Pulse.** Individual transmit pulses reflected off the surface of the earth and viewed by
1243 the ATLAS telescope are called reflected pulses. For a given transmit pulse, there may or may
1244 not be a reflected pulse. Not: received pulse, returned pulse.

1245

1246 **Photon Event.** Some of the energy in a reflected pulse passes through the ATLAS receiver
1247 optics and electronics. ATLAS detects and time tags some fraction of the photons that make up
1248 the reflected pulse, as well as background photons due to sunlight or instrument noise. Any
1249 photon that is time tagged by the ATLAS instrument is called a photon event, regardless of
1250 source. Not: received photon, detected photon.

1251

1252 **Reference Ground Track (RGT).** The reference ground track (RGT) is the track on the earth at
1253 which a specified unit vector within the observatory is pointed. Under nominal operating
1254 conditions, there will be no data collected along the RGT, as the RGT is spanned by GT2L and
1255 GT2R (which are not shown in the figures, but are similar to the GTs that are shown). During
1256 spacecraft slews or off pointing, it is possible that ground tracks may intersect the RGT. The
1257 precise unit vector has not yet been defined. The ICESat-2 mission has 1387 RGTs, numbered
1258 from 0001xx to 1387xx. The last two digits refer to the cycle number. Not: ground tracks, paths,
1259 sub-satellite track.

1260

1261 **Cycle Number.** Over 91 days, each of the 1387 RGTs will be targeted in the Polar Regions
1262 once. In subsequent 91-day periods, these RGTs will be targeted again. The cycle number
1263 tracks the number of 91-day periods that have elapsed since the ICESat-2 observatory entered the
1264 science orbit. The first 91-day cycle is numbered 01; the second 91-day cycle is 02, and so on.
1265 At the end of the first 3 years of operations, we expect the cycle number to be 12. The cycle
1266 number will be carried in the mid-latitudes, though the same RGTs will (in general) not be
1267 targeted more than once.

1268

1269 **Sub-satellite Track (SST).** The sub-satellite track (SST) is the time-ordered series of latitude
1270 and longitude points at the geodetic nadir of the ICESat-2 observatory. In order to protect the
1271 ATLAS detectors from damage due to specular returns, and the natural variation of the position
1272 of the observatory with respect to the RGT throughout the orbit, the SST is generally not the
1273 same as the RGT. Not: reference ground track, ground track.

1274

1275 **Ground Tracks (GT).** As ICESat-2 orbits the earths, sequential transmit pulses illuminate six
1276 ground tracks on the surface of the earth. The track width is approximately 10m wide. Each
1277 ground track is numbered, according to the laser spot number that generates a given ground
1278 track. Ground tracks are therefore always numbered with 1L on the far left of the spot pattern
1279 and 3R on the far right of the spot pattern. Not: tracks, paths, reference ground tracks, footpaths.

1280

1281 **Reference Pair Track (RPT).** The reference pair track is the imaginary line halfway between
1282 the planned locations of the strong and weak ground tracks that make up a pair. There are three
1283 RPTs: RPT1 is spanned by GT1L and GT1R, RPT2 is spanned by GT2L and GT2R (and may be
1284 coincident with the RGT at times), and RPT3 is spanned by GT3L and GT3R. Note that this is

1285 the planned location of the midway point between GTs. We will not know this location very
1286 precisely prior to launch. Not: tracks, paths, reference ground tracks, footpaths, pair tracks.

1287

1288 **Pair Track (PT).** The pair track is the imaginary line half way between the actual locations of
1289 the strong and weak ground tracks that make up a pair. There are three PTs: PT1 is spanned by
1290 GT1L and GT1R, PT2 is spanned by GT2L and GT2R (and may be coincident with the RGT at
1291 times), and PT3 is spanned by GT3L and GT3R. Note that this is the actual location of the
1292 midway point between GTs, and will be defined by the actual location of the GTs. Not: tracks,
1293 paths, reference ground tracks, footpaths, reference pair tracks.

1294

1295 **Pairs.** When considered together, individual strong and weak ground tracks form a pair. For
1296 example, GT2L and GT2R form the central pair of the array. The pairs are numbered 1 through
1297 3: Pair 1 is comprised of GT1L and GT1R, pair 2 is comprised of GT2L and GT2R, and pair 3 is
1298 comprised of GT3L and 3R.

1299

1300 **Along-track.** The direction of travel of the ICESat-2 observatory in the orbit frame is defined as
1301 the along-track coordinate, and is denoted as the +x direction. The positive x direction is
1302 therefore along the Earth-Centered Earth-Fixed velocity vector of the observatory. Each pair has
1303 a unique coordinate system, with the +x direction aligned with the Reference Pair Tracks.

1304

1305 **Across-track.** The across-track coordinate is y and is positive to the left, with the origins at the
1306 Reference Pair Tracks.

1307

1308 **Segment.** An along-track span (or aggregation) of PE data from a single ground track or other
1309 defined track is called a segment. A segment can be measured as a time duration (e.g. from the
1310 time of the first PE to the time of the last PE), as a distance (e.g. the distance between the
1311 location of the first and last PEs), or as an accumulation of a desired number of photons.
1312 Segments can be as short or as long as desired.

1313

1314 **Signal Photon.** Any photon event that an algorithm determines to be part of the reflected pulse.

1315

1316 **Background Photon.** Any photon event that is not classified as a signal photon is classified as a
1317 background photon. Background photons could be due to noise in the ATLAS instrument (e.g.
1318 stray light, or detector dark counts), sunlight, or mis-classified signal photons. Not: noise
1319 photon.

1320

1321 **h_{**}**. Signal photons will be used by higher-level products to determine height above the
1322 WGS-84 reference ellipsoid, using a semi-major axis (equatorial radius) of 6378137m and a
1323 flattening of 1/298.257223563. This can be abbreviated as ‘ellipsoidal height’ or ‘height above
1324 ellipsoid’. These heights are denoted by h; the subscript ** will refer to the specific algorithm
1325 used to determine that elevation (e.g. is = ice sheet algorithm, si = sea ice algorithm, etc...). Not:
1326 elevation.

1327

1328 **Photon Cloud**. The collection of all telemetered photon time tags in a given segment is the (or
1329 a) photon cloud. Not: point cloud.

1330

1331 **Background Count Rate**. The number of background photons in a given time span is the
1332 background count rate. Therefore a value of the background count rate requires a segment of PEs
1333 and an algorithm to distinguish signal and background photons. Not: Noise rate, background
1334 rate.

1335

1336 **Noise Count Rate**. The rate at which the ATLAS instrument receives photons in the absence of
1337 any light entering the ATLAS telescope or receiver optics. The noise count rate includes PEs
1338 due to detector dark counts or stray light from within the instrument. Not: noise rate,
1339 background rate, and background count rate.

1340

1341 **Telemetry band**. The subset of PEs selected by the science algorithm on board ATLAS to be
1342 telemetered to the ground is called the telemetry band. The width of the telemetry band is a
1343 function of the signal to noise ratio of the data (calculated by the science algorithm onboard
1344 ATLAS), the location on the earth (e.g. ocean, land, sea ice, etc...), and the roughness of the
1345 terrain, among other parameters. The widths of telemetry bands are adjustable on-orbit. The
1346 telemetry bandwidth is described in Section 7 or the ATLAS Flight Science Receiver Algorithms
1347 document. The total volume of telemetered photon events must meet the data volume constraint
1348 (currently 577 GBits/day).

1349

1350 **Window, Window Width, Window Duration**. A subset of the telemetry band of PEs is called a
1351 window. If the vertical extent of a window is defined in terms of distance, the window is said to
1352 have a width. If the vertical extent of a window is defined in terms of time, the window is said to
1353 have a duration. The window width is always less than or equal to the telemetry band.

1354

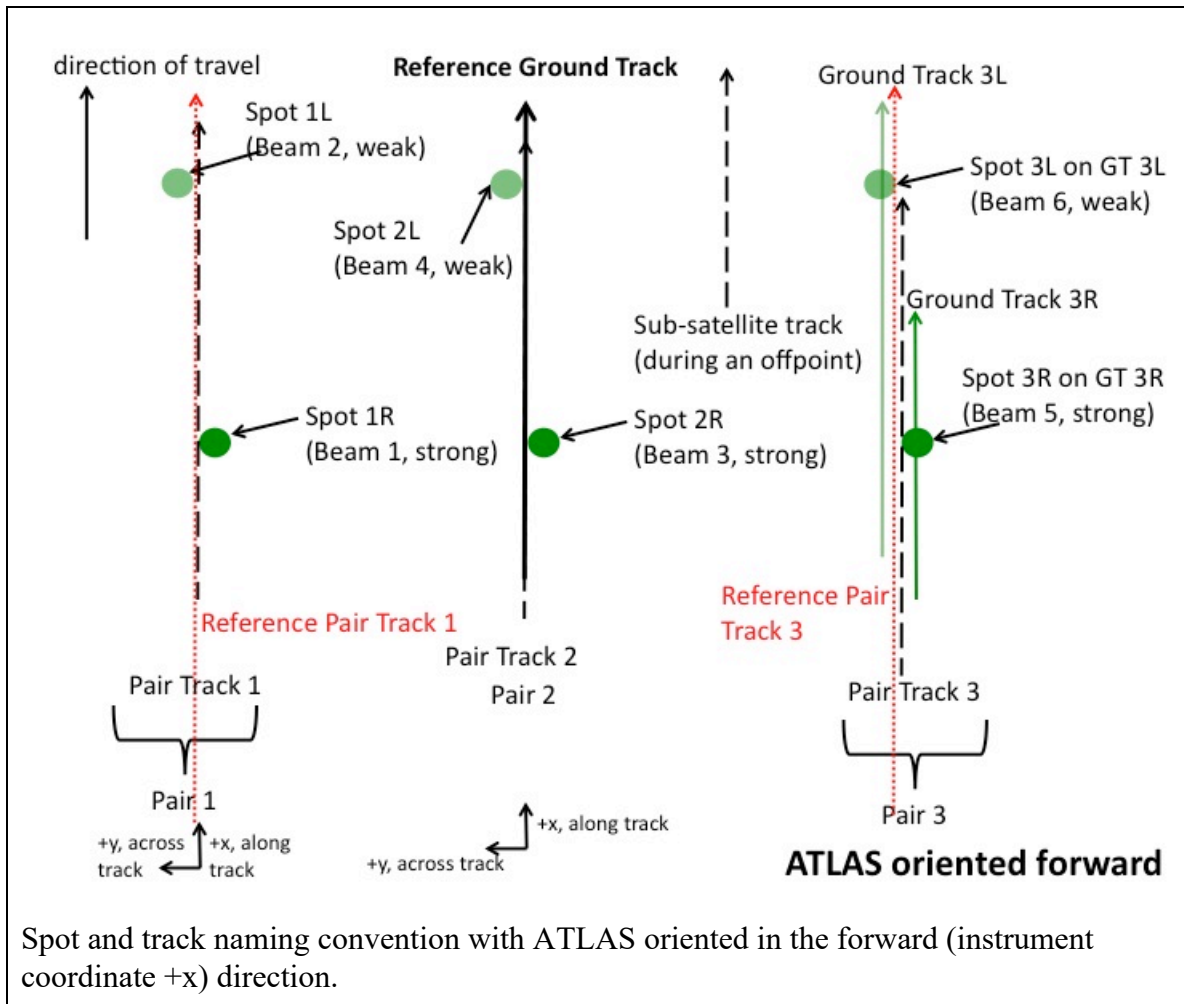
1355

1356

1357

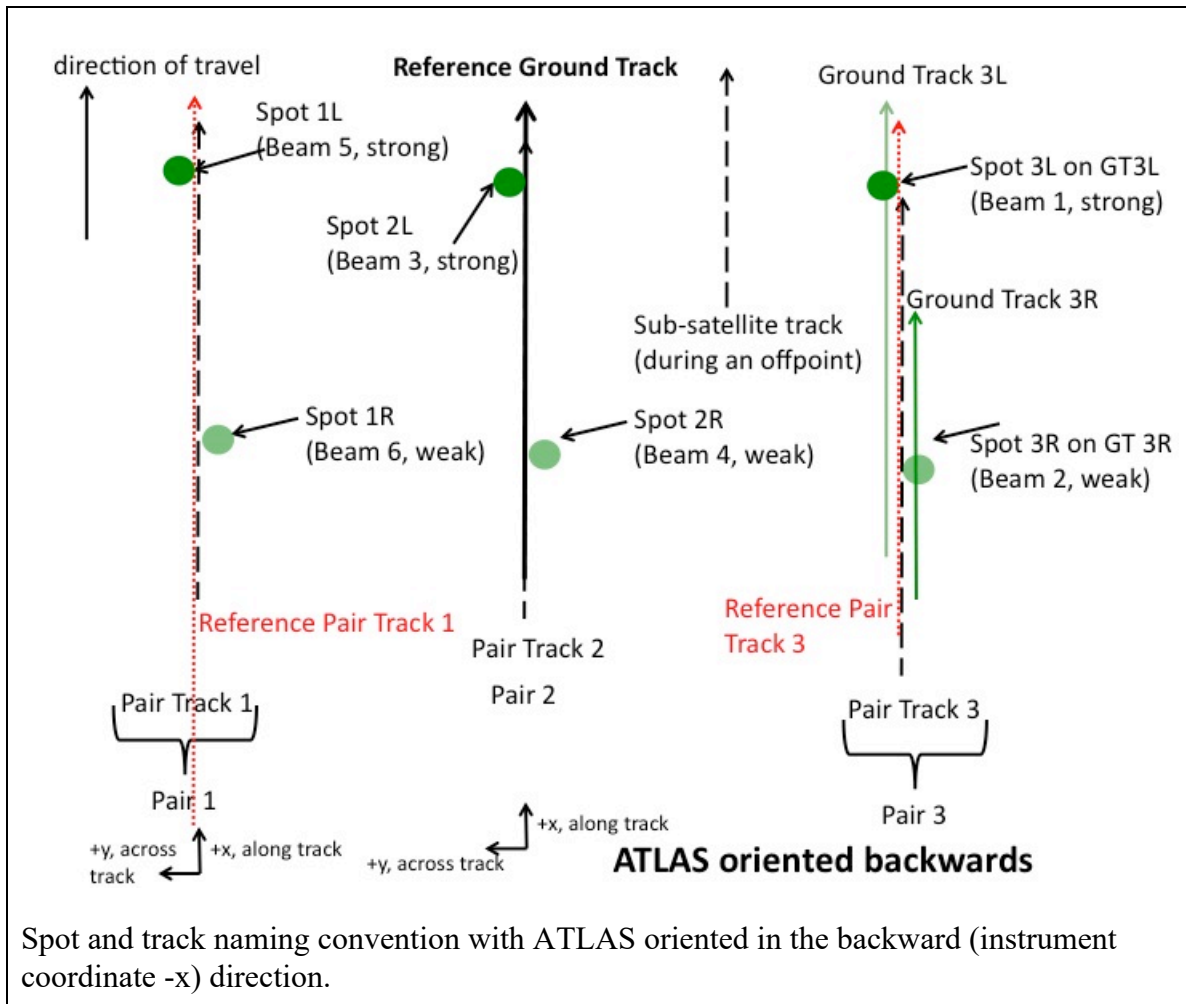
1358

Figure 6-1. Spots and tracks, forward flight



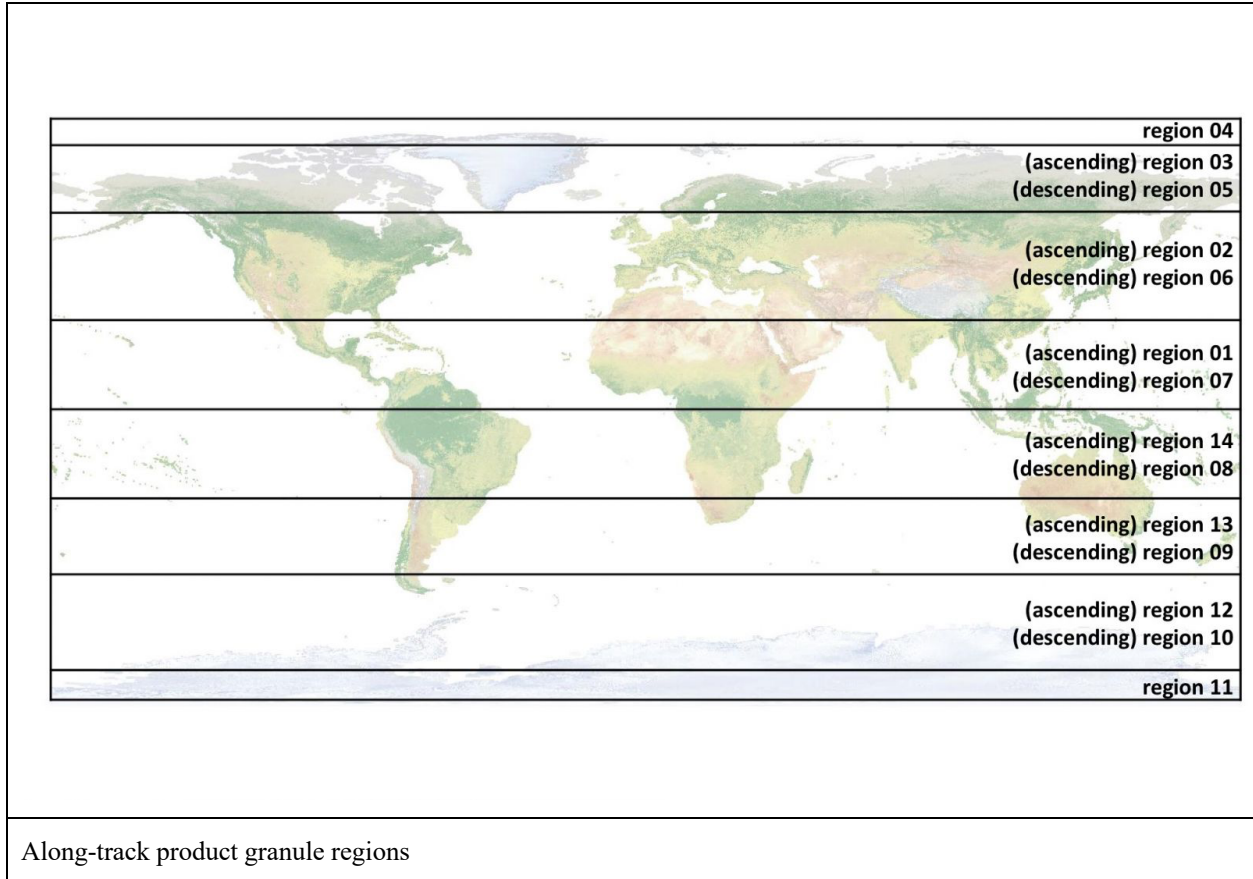
1359
 1360
 1361
 1362
 1363
 1364
 1365
 1366
 1367
 1368

Figure 6-2. Spots and tracks, backward flight



1369

Figure 6-3. Granule regions



1370 **7.0 BROWSE PRODUCTS**

1371 For each ATL11 data file, there will be eight figures written to an associated browse file. Two of
 1372 these figures are required and are located in the default group; default1 and default2. The browse
 1373 filename has the same pattern as the data filename, namely,
 1374 ATL11_ttttss_c1c2_rr_vVVV_BRW.h5, where tttt is the reference ground track, ss is the orbital
 1375 segment, c1 is the first cycle of data in the file, c2 is the last cycle of data in the file, rr is the
 1376 release and VVV is the version. Optionally, the figures can also be written to a pdf file.

1377

1378 Below is a discussion of the how the figures are made, with examples from the data file
 1379 ATL11_009403_0307_02_vU07.h5. Note that the figure numbering in this section is distinct
 1380 from that in the rest of the document; the figures shown here are labeled as they are in each
 1381 browse-product file.

1382

1383

1384

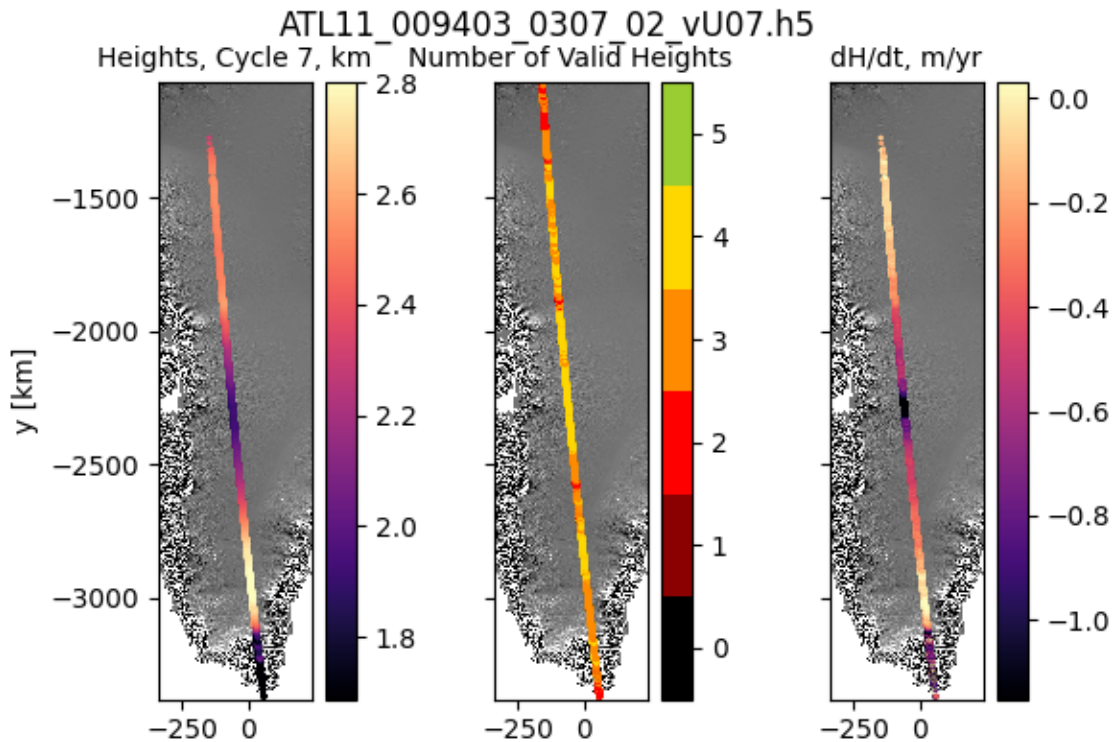


Figure 1. Height data, in km, from cycle 7 (1st panel). Number of cycles with valid height data (2nd panel). Change in height over time, in meters/year, cycle 7 from cycle 3 (3rd panel). All overlaid on gradient of DEM. x, y in km. Maps are plotted in a polar-stereographic projection with a central longitude of 45W and a standard latitude of 70N.

1385

1386

1387 The background for the three panels in Figure 1 is the gradient DEM in gray scale. It is shown in
 1388 a polar-stereographic projection with a central longitude of 45W (0E) and a standard latitude of
 1389 70N (71S), for the Northern (Southern) Hemisphere. The map is bounded by the extent of height
 1390 data plus a buffer. ATL11 heights (/ptx/h_corr) from all pairs of the latest cycle with valid data,
 1391 here cycle 7, are plotted in the first panel. The “magma” color map indicates the heights in km.
 1392 The limits on the color bar are set with the python scipy.stat.scoreatpercentile method at 5% and
 1393 95%. In the second panel are plotted the number of valid heights summed over all cycles at each
 1394 location. The color bar extends to the total number of cycles in the data file. The change in height
 1395 over time, dH/dt, is plotted in the third panel, in meters/year. dHdt is the change in height of the
 1396 last cycle with valid data from the first cycle with valid data (/ptx/h_corr) divided by the
 1397 associated times (/ptx/delta_time). Text of ‘No Data’ is printed in the panel if there is only one
 1398 cycle with valid data, or if the first and last cycles with valid data have no common reference
 1399 point numbers (/ptx/ref_pt). All plots are in x,y coordinates, in km. This figure is called
 1400 default/default1 in the BRW.h5 file.

1401

ATL11_009403_0307_02_vU07.h5

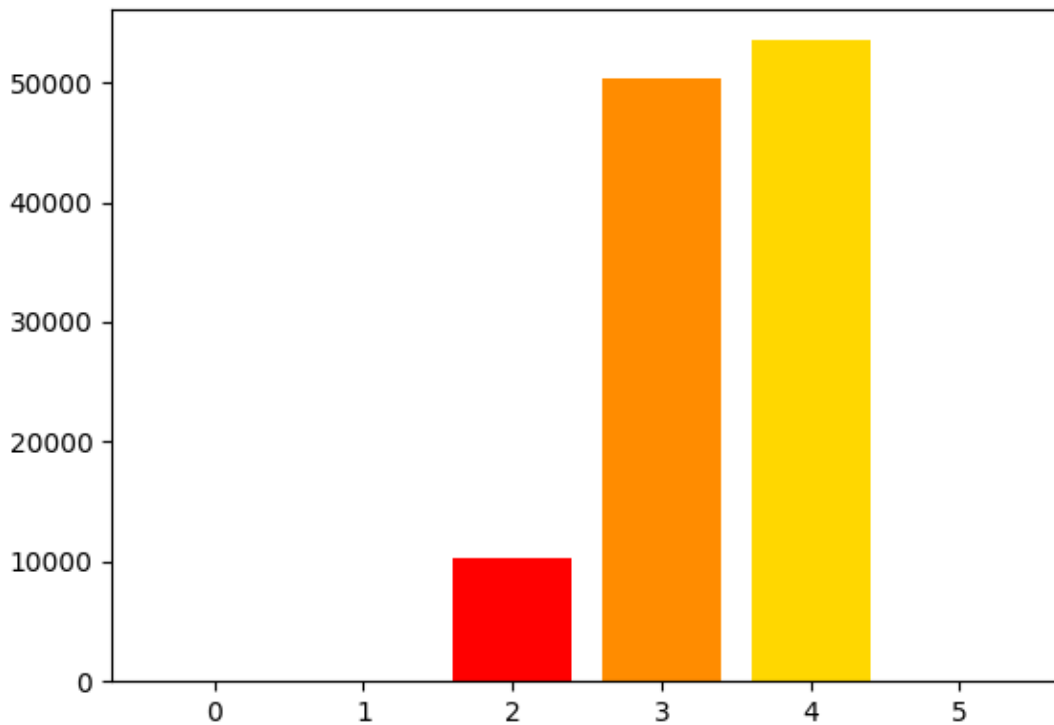


Figure 2. Histogram of number of cycles with valid height measurements, all beam pairs.

1402

1403

1404 A histogram of the number of valid height measurements (/ptx/h_corr) is in Figure 2. Valid
 1405 height data are summed across all cycles, for each reference point number (/ptx/ref_pt). The
 1406 color scale is from zero to the total number of cycles in the data file and matches those in Figure
 1407 1, 2nd panel. This figure is called validrepeats_hist in the BRW.h5 file.

1408

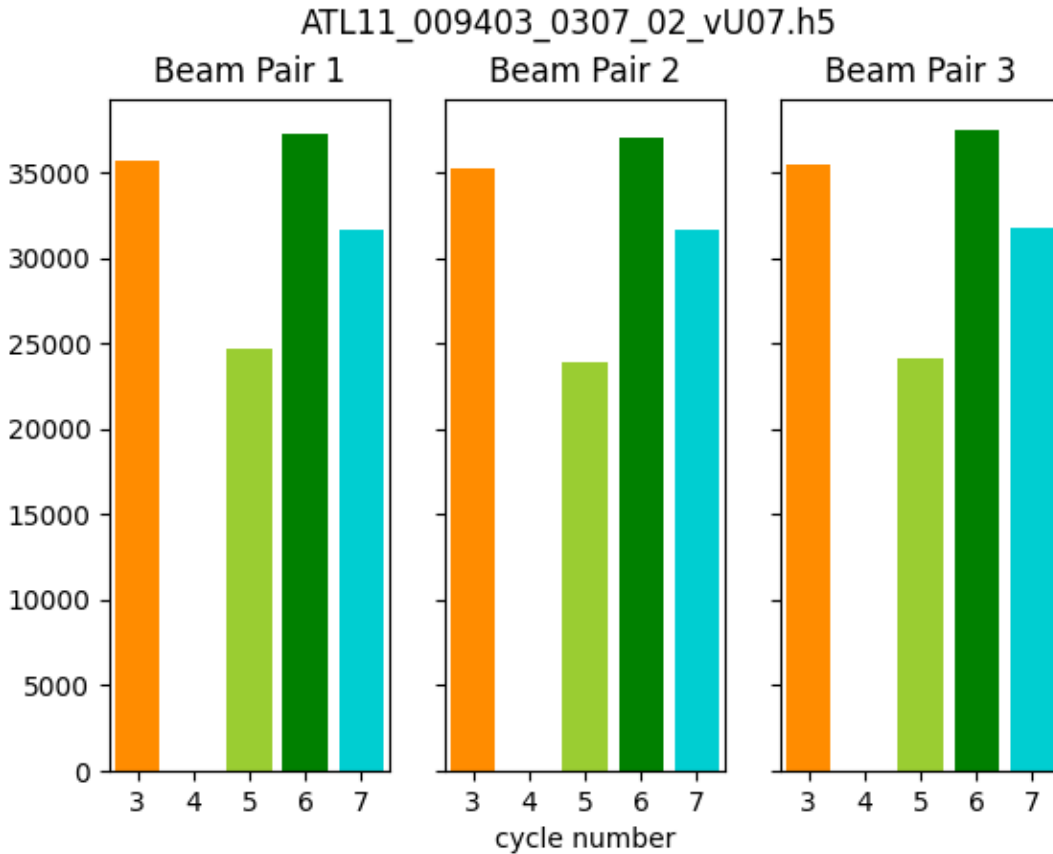


Figure 3. Number of valid height measurements from each beam pair.

1409

1410

1411 Histograms in Figure 3 show the number of valid heights (/ptx/h_corr) for each cycle, separated
 1412 by beam pair. The cycle numbers are color coded. This figure is called default/default2 in the
 1413 BRW.h5 file.

1414

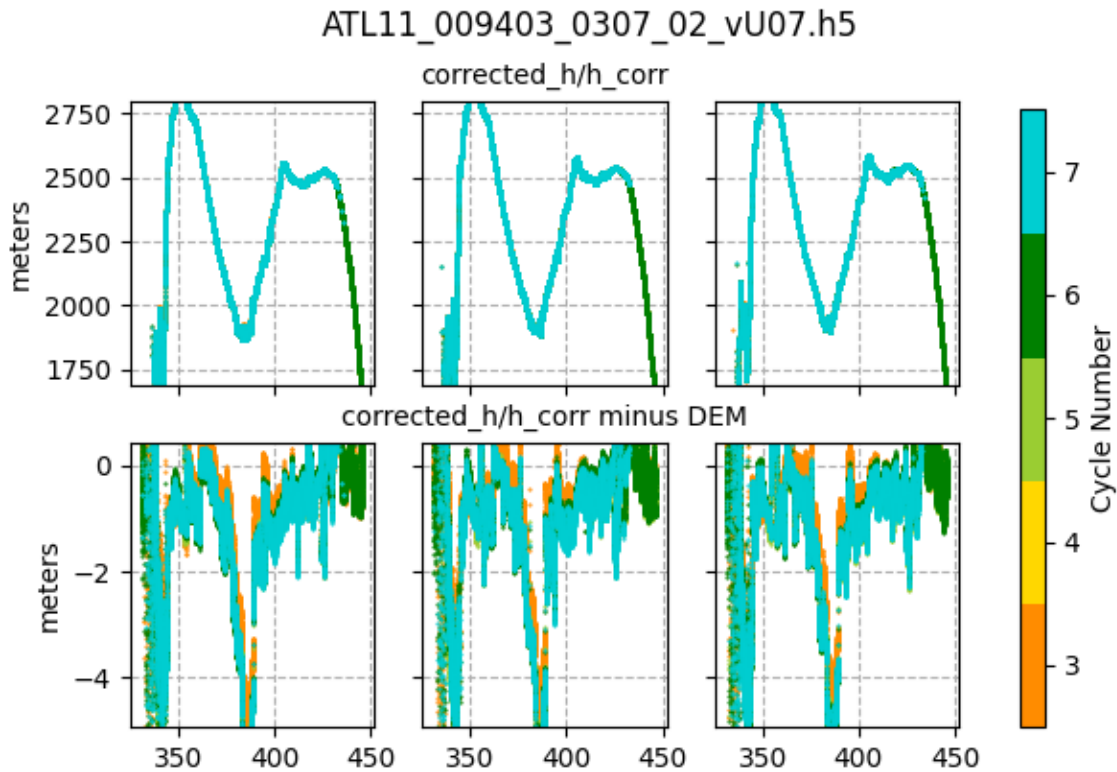


Figure 4. Top row: Heights, in meters, plotted for each beam pair: 1 (left), 2 (center), 3 (right). Bottom row: Heights minus DEM, in meters. Y-axis limits are scores at 5% and 95%. Color coded by cycle number. Plotted against reference point number/1000.

1415

1416

1417 There are six panels in Figure 4, with two rows and three columns. In the top row are plotted the
 1418 height measurements (/ptx/h_corr) for each beam pair, one pair per panel. In the bottom row are
 1419 plotted the same height measurements minus the collocated DEM (ref_surf/dem_h) values, one
 1420 pair per panel. The plots are color coded by cycle number, as in Figure 3. The heights are plotted
 1421 versus reference point number (/ptx/ref_pt) divided by 1000 for a cleaner plot. The y-axis is in
 1422 meters for both rows. The y-axis limits for the top and bottom rows are set separately, using the
 1423 python scipy.stats.scoreatpercentile method with limits of 5% and 95% for heights and height
 1424 differences, respectively. Text of 'No Data' is printed in a panel if there are no valid height data
 1425 for that pair. This figure is called h_corr_h_corr-DEM in the BRW.h5 file.

1426

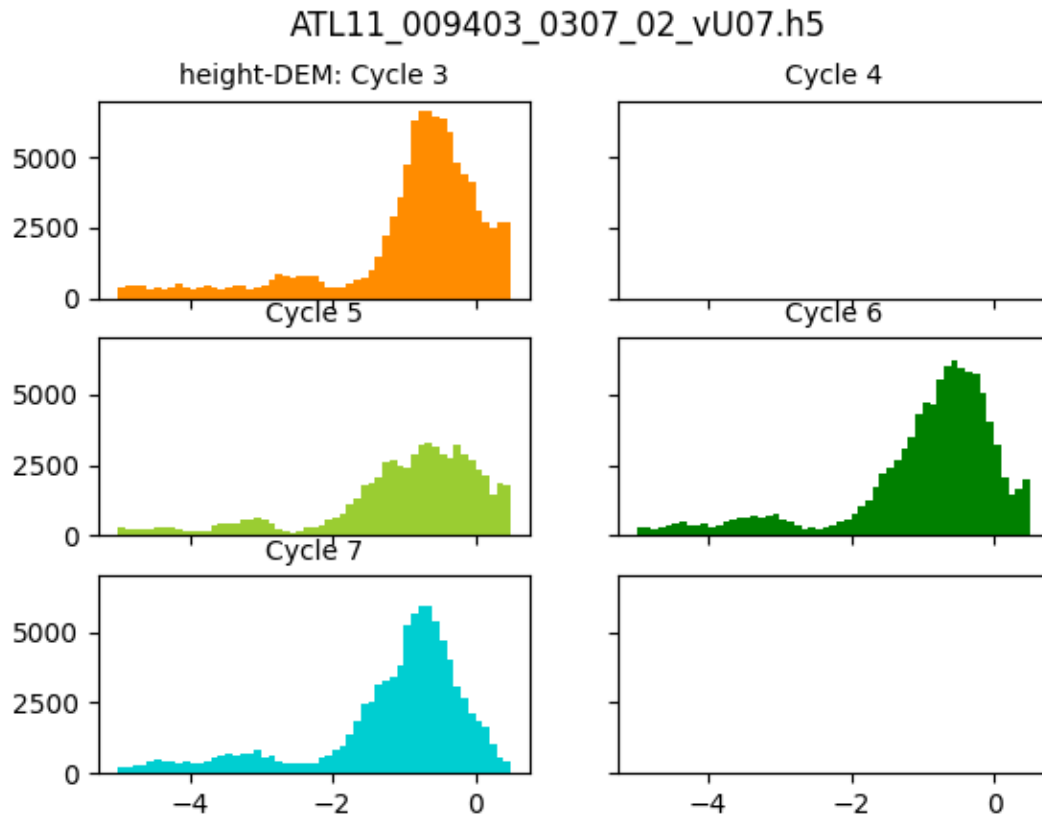


Figure 5. Histograms of heights minus DEM heights, in meters. One histogram per cycle, all beam pairs. X-axis limits are the scores at 5% and 95%.

1427

1428

1429

Figure 5 is associated with Figure 4. It is a multi-paneled figure, with the number of panels dependent on the number of cycles in the data file. Each panel is a histogram of the heights (/ptx/h_corr) minus collocated DEM heights (ref_surf/dem_h) color coded by cycle, the same as in Figures 3 and 4. The limits on the histograms are set using the python scipy.stats.scoreatpercentile method with limits of 5 and 95% for all cycles of data, the same values used in Figure 4 bottom row. This figure is called h_corr-DEM_hist in the BRW.h5 file.

1435

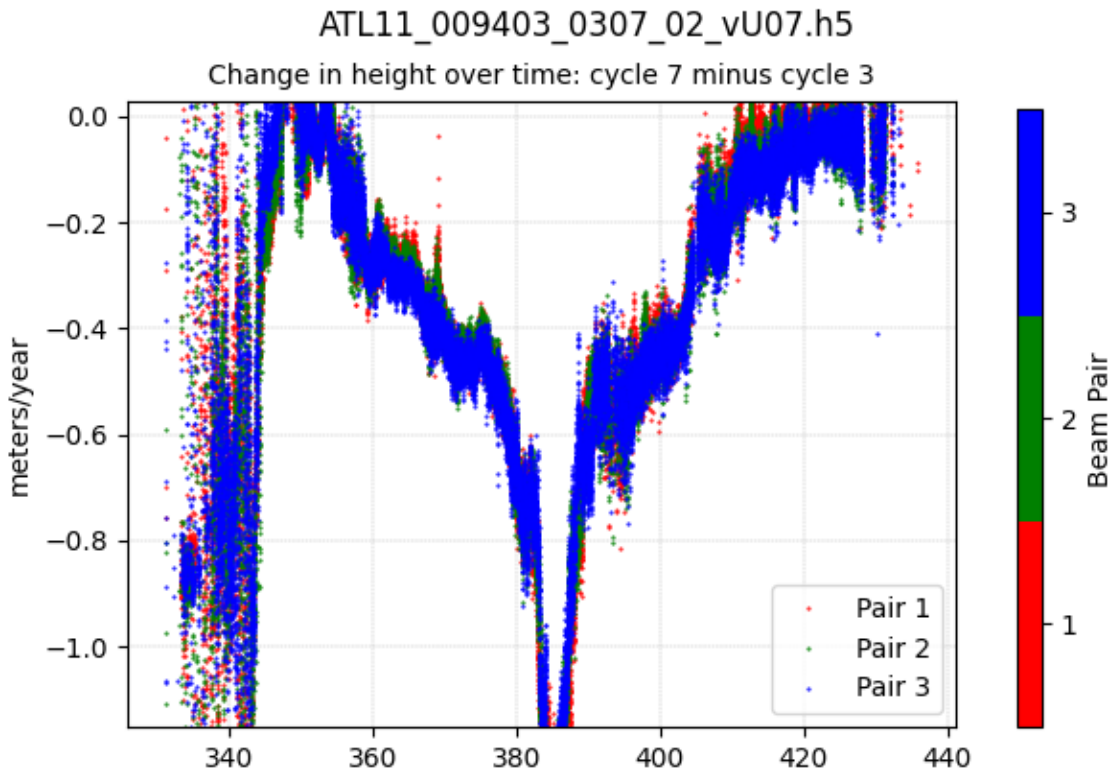


Figure 6. Change in height over time, dH/dt , in meters/year. dH/dt is cycle 7 from cycle 3. Color coded by beam pair: 1 (red), 2 (green), 3 (blue). Y-axis limits are scores at 5% and 95%. Plotted against reference point number/1000.

1436

1437

1438 The changes in height with time, dH/dt , in meters/year are plotted in Figure 6. The calculation
 1439 differences the first and last cycles with valid height data (`/ptx/h_corr`) divided by the associated
 1440 time differences (`/ptx/delta_time`). The change in heights for pair 1 are in red, for pair 2 are in
 1441 green and for pair 3 are in blue. The y-axis limits are set using the python
 1442 `scipy.stats.scoreatpercentile` method with limits of 5% and 95%. The x-axis is reference point
 1443 number (`/ptx/ref_pt`) divided by 1000 for a cleaner plot. Text of 'No Data' is printed in the panel
 1444 if there is only one cycle with valid data, or if the first and last cycles with valid data have no
 1445 common reference point numbers. This figure is called `dHdt` in the `BRW.h5` file.

1446

1447

1448

Glossary/Acronyms

ASAS	ATLAS Science Algorithm Software
ATBD	Algorithm Theoretical Basis Document
ATLAS	ATLAS Advance Topographic Laser Altimeter System
CDF	Cumulative Distribution Function
DEM	Digital Elevation Model
GSFC	Goddard Space Flight Center
GTs	Ground Tracks
ICESat-2	Ice, Cloud, and Land Elevation Satellite-2
IKR	I Know, Right?
MABEL	Multiple altimeter Beam Experimental Lidar
MIS	Management Information System
NASA	National Aeronautics and Space Administration
PE	Photon Event
POD	Precision Orbit Determination
PPD	Precision Pointing Determination
PRD	Precise Range Determination
PSO	ICESat-2 Project Science Office
PTs	Pair Tracks
RDE	Robust Dispersion Estimate
RGT	Reference Ground Track
RMS	Root Mean Square
RPTs	Reference Pair Tracks

RT	Real Time
SCoRe	Signature Controlled Request
SIPS	ICESat-2 Science Investigator-led Processing System
TLDR	Too Long, Didn't Read
TBD	To Be Determined

1449

References

1450 Brunt, K.M., H.A. Fricker and L. Padman 2011. Analysis of ice plains of the Filchner-Ronne Ice
1451 Shelf, Antarctica, using ICESat laser altimetry. *Journal of Glaciology*, **57**(205): 965-975.

1452 Fricker, H.A., T. Scambos, R. Bindshadler and L. Padman 2007. An active subglacial water
1453 system in West Antarctica mapped from space. *Science*, **315**(5818): 1544-1548.

1454 Schenk, T. and B. Csatho 2012. A New Methodology for Detecting Ice Sheet Surface Elevation
1455 Changes From Laser Altimetry Data. *Ieee Transactions on Geoscience and Remote Sensing*,
1456 **50**(9): 3302-3316.

1457 Smith, B., H.A. Fricker, N. Holschuh, A.S. Gardner, S. Adusumilli, K.M. Brunt, B. Csatho, K.
1458 Harbeck, A. Huth, T. Neumann, J. Nilsson and M.R. Siegfried 2019a. Land ice height-retrieval
1459 algorithm for NASA's ICESat-2 photon-counting laser altimeter. *Remote Sensing of*
1460 *Environment*: 111352.

1461 Smith, B.E., H.A. Fricker, I.R. Joughin and S. Tulaczyk 2009. An inventory of active subglacial
1462 lakes in Antarctica detected by ICESat (2003-2008). *Journal of Glaciology*, **55**(192): 573-595.

1463 Smith, B.E., D. Hancock, K. Harbeck, L. Roberts, T. Neumann, K. Brunt, H. Fricker, A.
1464 Gardner, M. Siegfried, S. Adusumilli, B. Csatho, N. Holschuh, J. Nilsson and F. Paolo 2019b.
1465 Algorithm Theoretical Basis Document for Land-Ice Along-track Product (ATL06). Goddard
1466 Space Flight Center.

1467